# Molecular mechanism(s) of growth phase transitions

A thesis submitted for the partial fulfillment of the degree of

**Master of Science**

as part of the Integrated Ph.D. program

(Biological Sciences)

by

**Rashi Aggarwal**


**Molecular Mycology Laboratory**

**Molecular Biology and Genetics Unit**

**Jawaharlal Nehru Center for Advanced Scientific Research**

**(A deemed university)**

**Jakkur, Bangalore 560064.**

**March 2019**

# DECLARATION

I hereby declare that the work described here in this thesis entitled **'Molecular mechanism(s) of growth-phase transitions'** has originally been carried out by myself under the guidance and supervision of Kaustuv Sanyal, Professor, Molecular Biology and Genetics Unit, Jawaharlal Nehru Centre for Advanced Scientific Research, Bangalore-560064, India.

In keeping with the general practice of reporting scientific observations, due acknowledgments have been made wherever the work described has been based on findings of other investigators. Any omission, which might have occurred by oversight or misjudgment, is regretted.

Rashi Aggarwal

Date:

# CERTIFICATE

This is to certify that this thesis entitled '**Molecular mechanism(s) of growth-phase transitions**' submitted by Rashi Aggarwal towards the Integrated Ph.D. Program, as part of Project for MS, at Jawaharlal Nehru Centre for Advanced Scientific Research, was based on the studies carried out by her under my supervision and guidance.

Prof. Kaustuv Sanyal

Date:

# ACKNOWLEDGMENT

The present study has been possible due to contributions from many people. I take this opportunity to thank them.

First and foremost, I am thankful to my research supervisor, Prof. Kaustuv Sanyal. He gave me the opportunity to work on this project. He has been very patient with me and provided his valuable inputs as and when required. Moreover, he gave me the space to plan my experiments. His words have always inspired me to work harder and have helped me greatly in the overall development of my personality.

Next, I wish to express my thanks to Honorary Faculty Fellow in MBGU, Dr. G. R. Ramesh. He was my first mentor in JNCASR. He taught me basic microbiology techniques and lab ethics which have helped me immensely. He is a phenomenal teacher, and his teachings will stay with me throughout my academic career and beyond. Time spent in his lab with my batchmates (Chhavi, Shubham, Irine, Ankit, Saheli and Kuladeep) will be a cherished memory. I am thankful to Prof. Sheeba Vasu and her students for taking a laboratory course. She and her students helped me and my batchmates to do several fun experiments aimed at understanding circadian rhythms and fly genetics. These experiments helped me understand how to approach a research problem and how to analyze a given data in the best possible way. I am especially thankful to Abhilash as he has truly been my 'Statistics Guru'. His classes taught me how to ask a research question. He has always extended his help whenever required.

I am also thankful to Prof. Hemalatha Balaram and Dr. Meher K. Prakash under whom I did my first lab rotation. I had many learning experiences in their labs, and they have always counseled me whenever required. I am grateful to all their lab members. They have been good friends and have taught me biotechnology and bioinformatic techniques/tools. I am especially thankful to Lakshmeesha, Aparna and Asutosh. They have guided me not just as friends but as teachers too.

I want to express my gratitude towards our president, Prof. V. Nagaraja, and our chairman, Prof. Uday Kumar Ranga for providing all the necessary facilities in the department and encouraging me throughout. Also, I am grateful to the faculty members of Molecular Biology and Genetics Unit (MBGU) Prof. Anuranjan Anand, Prof. Maneesha Inamdar, Prof. Tapas Kundu, Prof. Namita Surolia, Prof. Ravi Manjithaya and Dr. James

Chelliah for the course work they took during my masters. Their classes have been enjoyable and enlightening.

Next, I was fortunate to be a part of the Molecular Mycology Lab. All the members of the lab have extended their help and inputs whenever required. The project was initiated by Dr. Laxmi Rai and carried forward by Rima. Their contributions to the project laid forward the foundation for me to carry further. I am especially thankful to Rima who gave me the opportunity to gain knowledge about the skills required for my work from her. She has guided me at every step of this project, and without her, this project would not have matured into its present form. I am thankful to her and Dr. Neha for proofreading this thesis. It has been an incredible learning experience with them. Shreyas has helped me with microscopy and immuno-pulldown experiment. His continuous guidance and constructive criticism motivated me to learn from experimental failures. Priya J has been extremely patient with me. Discussions with her have always been inspiring and helped me in developing both as a researcher and a human. Satya has been a good friend in the lab. I am grateful to him for teaching me all the basics of microscopy. Priya B and Dr. Vikas have showered enormous love and care on me. Other members of the lab including Dr. Lakshmi, Dr. Hashim, Dr. Shweta, Dr. Ashwathy, Sundar, Krishnendu, Prathamesh, and Padmalaya have also extended their help whenever required. I am thankful to Abhijit and Promit for all the fun sessions I had with them. Nagaraj in the lab maintained all the instruments and provided glasswares enabling me to work.

I have been very fortunate to have many good friends in JNCASR. Two of them, Chhavi and Vijay Kumar MJ deserves a special mention. They have always been very supportive and kind to me. I have celebrated both my achievements and failures with them. They have contributed to this project by patiently listening to me whenever I wished to discuss. I will cherish the moments I have spent with them forever.

Lastly, no words will ever be enough to thank my parents. They are the powerhouse of all my energy. Everything I have achieved academically and the person I have grown up to be is because of their constant efforts. I am thankful to them for weathering my minor crisis of confidence. My brother, Rishabh, have also played an instrumental role in shaping my personality.

Rashi

# Table of contents

# List of figures



# List of tables

# ABBREVIATIONS

| | |
|---|---|
| CGD | Candida Genome Database |
| DNA | Deoxyribonucleic acid |
| DTT | Dithiothreitol |
| EDTA | Ethylenediaminetetraacetic acid |
| EGTA | Ethyleneglycoltetraacetic acid |
| EtBr | Ethidium Bromide |
| GUT | Gastrointestinally Induced Transition |
| h | Hour |
| Ig | Immunoglobin |
| kb | kilobasepairs |
| kDa | Kilodalton |
| Mb | Megabasepairs |
| µg | Microgram |
| min | Minutes |
| µl | Microlitre |
| µm | Micrometer |
| ml | Milliliter |
| mM | Millimolar |
| ng | Nanogram |
| ORF | Open Reading Frame |
| PAGE | Polyacrylamide Gel Electrophoresis |
| PBS | Phosphate buffered saline |
| PCR | Polymerase Chain Reaction |
| SDS | Sodium Dodecyl Sulphate |
| °C | Degree Celsius |
| Δ | Deleted |
| bp | Base pair |
| GFP | Green fluorescent protein |
| MNase | Micrococcal nuclease |
| NAT | Nourseothricin acetyltransferase |
| rpm | Revolutions per minute |

**The art of life is constant readjustment to our surroundings.**

**- Okakuru Kakuzo**

# 1. INTRODUCTION

## 1.1 Fungal molecular pathogenesis: What and Why

Fungi play several vital roles in the ecosystem including driving the global carbon cycle, sustainment of agricultural and plant biodiversity through mycorrhizal associations and other benefits including food, beer, and life-saving antibiotics for mankind (KENDRICK 2000). However, they can also be pathogens of plants and animals. Interestingly, fungal infections are relatively rare in mammals suggesting that mammals have complex defense mechanisms and fungal species failed to develop ways to counteract them (CRAMER AND PERFECT 2009). Mammals exhibit remarkable fungal resistance, and a thorough knowledge of these mechanisms is critical for the understanding of fungal pathogenesis in humans. Several inherent attributes of mammals contribute to this resistance. First, mammals have a core body temperature that ranges from 37°C to 39°C which is non-permissive for most fungal species. Second, body fluids of mammals are alkaline in nature whereas most fungi prefer growth in slightly acidic to neutral pH. Finally, complex innate and adaptive immune systems of mammalian host prevent fungal growth (CRAMER AND PERFECT 2009). A fungus must be able to overcome these barriers to cause infection successfully.

Recent advances in medical technologies such as the use of prosthetics, chemotherapy for cancer treatment and use of immunosuppressive drugs for organ transplantations have led to an unintended consequence of increased fungal infections (MCNEIL *et al.* 2001). Cramer Jr. and Perfect described the fungal disease as *Goldilocks paradigm* of host immunity (CRAMER AND PERFECT 2009). Infections occur when there are host immune imbalances - either too little (invasive mycoses) or too much (immune reconstitution syndrome; IRS). Recently, there has been a great stride in the development of antifungals, but it is inevitably coupled with increased drug resistance. Most antifungals target cellular functions which require high specificity and may lead to emergence of resistance. Inhibition of growth and virulence factors in fungal cells is a good alternative for new antifungals (PIERCE AND LOPEZ-RIBOT 2013). Hence, a better understanding of fungal pathogenesis is essential to develop novel treatment and preventive strategies.

## 1.2 Evolution of fungal morphologies and virulence in *Candida* spp.

Many pathogenic (*Candida albicans*) and non-pathogenic (*Saccharomyces cerevisiae*) fungal species possess the ability to alter their morphology. Fungal morphologies have been studied intensely and, the discovery that most human fungal pathogens undergo

morphological changes suggested an association with virulence (SAN-BLAS *et al.* 2000; KLEIN AND TEBBETS 2007).

Fungal species grow mainly in three morphologies: yeast, pseudohyphae, and hyphae (**Figure 1**). Yeast cells are round to oval and exhibit both axial and bipolar budding patterns. Pseudohyphae and hyphae are the filamentous forms as they grow in a polarized manner, are elongated and are chains of cells attached to each other. Pseudohyphal cells are ellipsoid in shape with constrictions at the septal junctions. In contrast, hyphae have parallel walls without any constrictions. Even though phenotypically, pseudohyphae appear similar to hyphae they share more properties with yeast cells and are thus better described as elongated, attached yeast cells (SUDBERY *et al.* 2004). Additionally, the conventional views are that yeast cells are essential for dissemination of the infection, while the filamentous forms can penetrate the host barrier and damage the tissues.

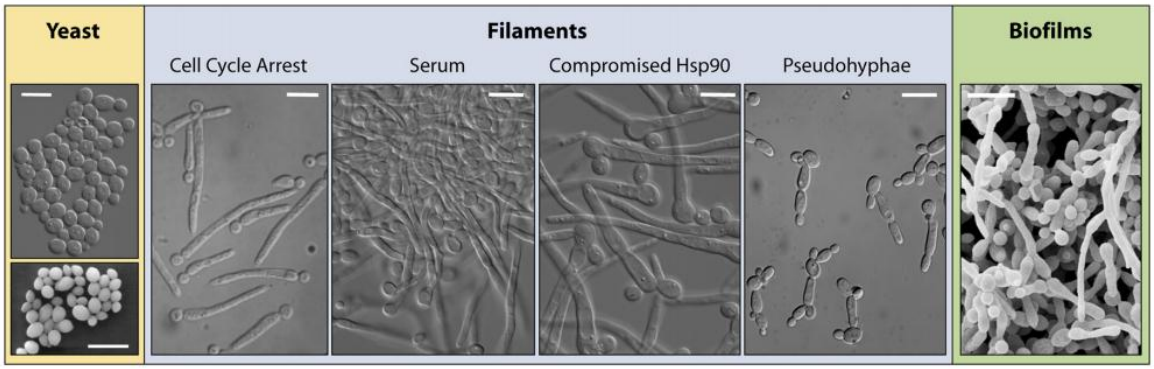


**Figure 1 Different morphological forms of *C. albicans*.**
*C. albicans* can exist in both yeast and filamentous forms. Also, it can form biofilms which are a complex community of multiple cell types. Differential interference contrast (DIC) images (top left) and scanning electron microscopy (SEM) images (bottom left) of yeast form are shown. The filaments depicted (middle panels) are induced by different environmental cues: cell cycle arrest upon the depletion of CDC5, 10% serum at 37°C, compromised Hsp90 function by treatment with geldanamycin, and pseudohyphae produced in the medium at pH 6.0 at 35°C. Biofilm image (right) is an SEM image of a mature (48h) biofilm composed of yeast and filamentous cells. Scale bars, 10 μm. [Image reproduced from (SHAPIRO *et al.* 2011)]

Mammalian host appeared long after fungi; hence it is interesting to study morphological evolution of fungal pathogens under selective host pressures. Evidence from studies done on *Candida* species strongly suggests that morphology may have evolved in a stepwise manner from yeast to pseudohyphae to hyphae [(CARLISLE *et al.* 2009; THOMPSON *et al.* 2011), **Figure 2**]. Moreover, a common transcriptional mechanism specifies the shift from yeast to pseudohyphal to hyphal morphology in a dosage-dependent manner (CARLISLE

*et al.* 2009). Consistent with this model of step-wise evolution, many *Candida* species can form yeast and pseudohyphae. However, true hyphae are formed only by closely related *Candida spp.* (*C. tropicalis*, *C. dubliniensis*, and *C. albicans*). Recently, *Candida auris*, a newly evolved *Candida* species have also been shown to form hyphae (**Table 1**)

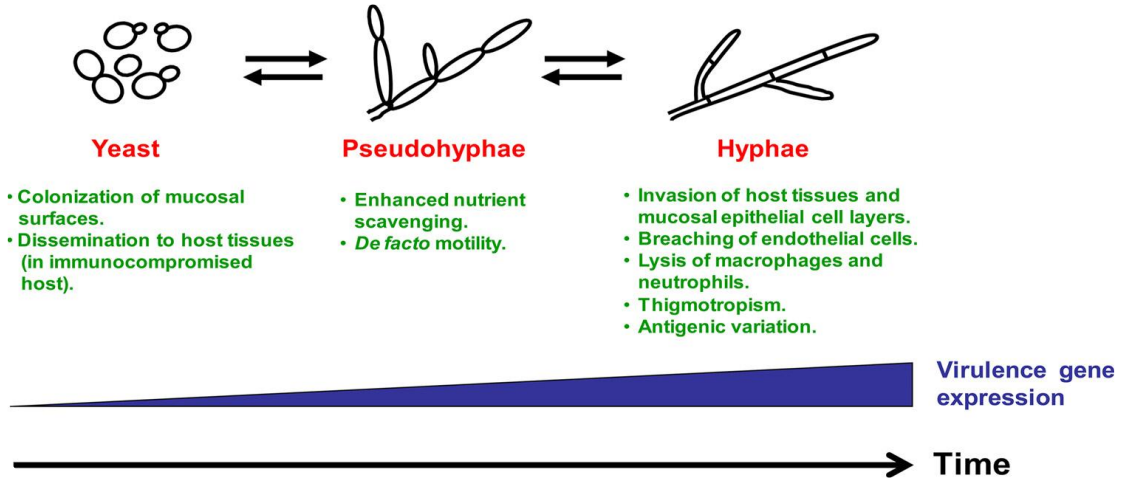


**Figure 2 Model for evolution of morphology and virulence in *Candida* spp.**
Stepwise evolution from yeast to pseudohyphae to hyphae is associated with increased virulence-associated gene expression. Pseudohyphae may have evolved to possess weaker versions of several virulence properties related to hyphae. Moreover, it is important to note that these transitions are reversible, and the yeast form has also evolved to play several important roles in the virulence process. [Image reproduced from (THOMPSON *et al.* 2011)]

**Table 1 Morphologies of major pathogenic *Candida* species**

| Species | Morphology |
|---|---|
| ***C. glabrata*** | Yeast, pseudohyphae |
| ***C. lusitaniae*** | Yeast, pseudohyphae |
| ***C. guilliermondii*** | Yeast, pseudohyphae |
| ***C. parapsilosis*** | Yeast, pseudohyphae |
| ***C. tropicalis*** | Yeast, pseudohyphae, hyphae |
| ***C. dubliniensis*** | Yeast, pseudohyphae, hyphae |
| ***C. albicans*** | Yeast, pseudohyphae, hyphae |
| ***C. auris*** | Yeast, pseudohyphae, hyphae (YUE *et al.* 2018) |

However, the quite convincing stepwise yeast-pseudohyphae-hyphae evolution model in *C. albicans* is challenged by the reductive evolution model in *C. dubliniensis* which involves loss of hypha-specific virulence factors *(JACKSON et al. 2009)*. This implies that *C. dubliniensis*, unlike *C. albicans*, has lost the genomic capacity to form hyphae and key pathogenic functions. Hence, our knowledge about the evolutionary relationship between

morphology and virulence is limited. Studies on morphogenetic processes in fungal pathogens such as *C. albicans*, one of the most successful pathogens, may shed some light on this. Further, the cross-species comparative analysis may allow us to arrive at a common evolutionary model that can describe co-evolution of morphology and virulence for all pathogenic *Candida* species.

### 1.3 *C. albicans*: An opportunistic commensal pathogen

**Taxonomic position**

Domain: Eukarya
Kingdom: Fungi
Phylum: Ascomycota
Subphylum: Saccharomycotina
Class: Saccharomyces
Order: Saccharomycetales
Family: Debaromycetaceae
Genus: *Candida*
Species: *albicans*

*Candida* sp. causes a deadly fungal infection called candidiasis. Candidiasis has a high mortality rate that ranges from 46-75%. Moreover, *Candida* now ranks as the third most common cause of invasive bloodstream infections in hospitals in the United States (PENDRAK *et al.* 2004). *C. albicans* is the most common species found in clinical settings; it accounts for more than 50% cases of candidiasis (LIM *et al.* 2012). As a commensal, it colonizes the mucocutaneous, gastrointestinal and genitourinary tracts of the human body. When the host immune system is compromised, it can become pathogenic. Many factors contribute to this remarkable opportunistic infection causing ability of *C. albicans* which includes expression of host recognition biomolecules (adhesins), morphological transitions, secretion of aspartyl proteases and phospholipases (NOBLE *et al.* 2017).

Several hallmarks of *C. albicans* biology have led to its emergence as a model system complementary to *S. cerevisiae* and *S. pombe (LEGRAND et al. 2019).* Unlike *S. pombe* and *S. cerevisiae*, *C. albicans* was believed to undergo asexual reproduction only. However, the discovery of Mating-Type Like locus (MTL locus) with two alleles **a** and $\alpha$ led to the identification of a rare parasexual cycle. Strains homozygous at this locus (white cells) can switch to form mating -competent opaque cells which can fuse with an opposite mating type opaque cell to give tetraploid cells. These tetraploid cells can undergo concerted chromosome loss to return to the diploid state, thus completing a parasexual cycle (HULL *et al.* 2000; MAGEE AND MAGEE 2000; MILLER AND JOHNSON 2002).

*C. albicans* has a haploid genome size of 16 Mb which is distributed amongst eight chromosomes (1-7 and R) (CHIBANA *et al.* 2005). Furthermore, it belongs to the CTG clade of Ascomycota since there exists a translational bias, wherein CTG often uses a non-standard genetic code that is instead of leucine it codes for serine. Due to this reason, all the fluorescent markers used in this study are codon optimized (*Candida Genome Database*). The genome of *C. albicans* exhibits a high degree of plasticity which includes chromosomal rearrangements, aneuploidy, and loss of heterozygosity. Such an organization enables the fungus to survive in stressful environments such as antifungal drug exposure (SELMECKI *et al.* 2010). Further insights into the lifestyle of this pathogenic yeast can enhance our understanding of eukaryotic genome biology in general as well as mechanisms of fungal pathogenesis.

One of the most crucial virulence traits of *C. albicans* is its ability to exist in diverse morphological forms. It exhibits remarkable phenotypic plasticity as, apart from three classical forms (yeast, pseudohyphae and, hyphae), it can exist in several more elongated yeast-like cell types including chlamydospore, opaque, grey and GUT (NOBLE *et al.* 2017). Features of these cell types are summarized in **Table 2**. The present study focuses on yeast, pseudohyphae and hyphal forms of *C. albicans*.

Three wild-type isolates of *C. albicans* commonly used in the laboratory are SC5314, WO-1, and P37005 (LOCKHART *et al.* 2002). These strains are sensitive to nourseothricin and hygromycin B antibiotics. Hence, they are routinely used as selectable markers for transformations (*Candida Genome Database*). To further facilitate genetic manipulations auxotrophic markers have been deleted in wild-type strains. SN148 is a derivative of SC5314 in which *URA3, ARG4, LEU2,* and *HIS1* genes are deleted (NOBLE AND JOHNSON 2005). The present study utilizes both SC5314 and SN148 strains of *C. albicans*.

**Table 2 Features of *C. albicans* cell types**

| | Inducing Conditions | Morphological Features | Function |
|---|---|---|---|
| **White** | Default | Round-Oval | Virulence; commensalism; biofilm formation |
| **Hypha** | 37°C, *N*-acetylglucosamine, serum, immersion in agar, hypoxia, hypercarbia and alkaline pH | Elongated tube | Biofilm formation; Induced endocytosis; active penetration of host epithelial cells; virulence (mouth, vagina and bloodstream models) |
| **Pseudohypha** | Hypha-inducing cues | Elongated ellipsoid | Virulence, biofilm formation |
| **Opaque** | *N*-acetylglucosamine, hypercarbia and acidic pH | Ellipsoid with surface pimples | Mating, High fitness in a neonatal mouse skin colonization model |
| **Grey** | Nutrient abundance | Smallest and ellipsoid | High fitness in an *ex vivo* tongue infection model |
| **Chlamydospore** | Nutrient scarcity, hypoxia | Round and thick cell wall | Unknown |
| **GUT** | Unknown | Ellipsoid | High fitness in a mouse gastrointestinal commensalism model |

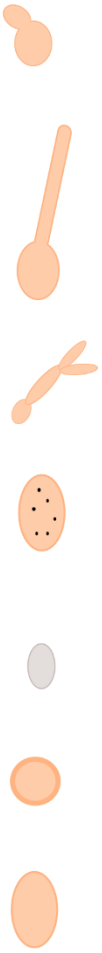

## 1.4 Morphological transitions

*C. albicans* exhibit enormous morphological plasticity enabling it to transit in different morphological forms. Commonly observed morphological transitions are summarized in **Figure 3**. The ability of *C. albicans* to shift from commensal to pathogenic lifestyle is partly attributed to its ability to undergo transition from yeast state to filamentous forms in response to host factors and stress conditions. This switching provides cells with the flexibility that allow adaptation of organism in hostile conditions (NOBLE *et al.* 2017). Moreover, morphological switching leads to profound changes in genome-wide expression profiles. In the present study, we aimed at understanding yeast to hyphae and planktonic to biofilm transitions since they have been proved to be important for pathogenicity.

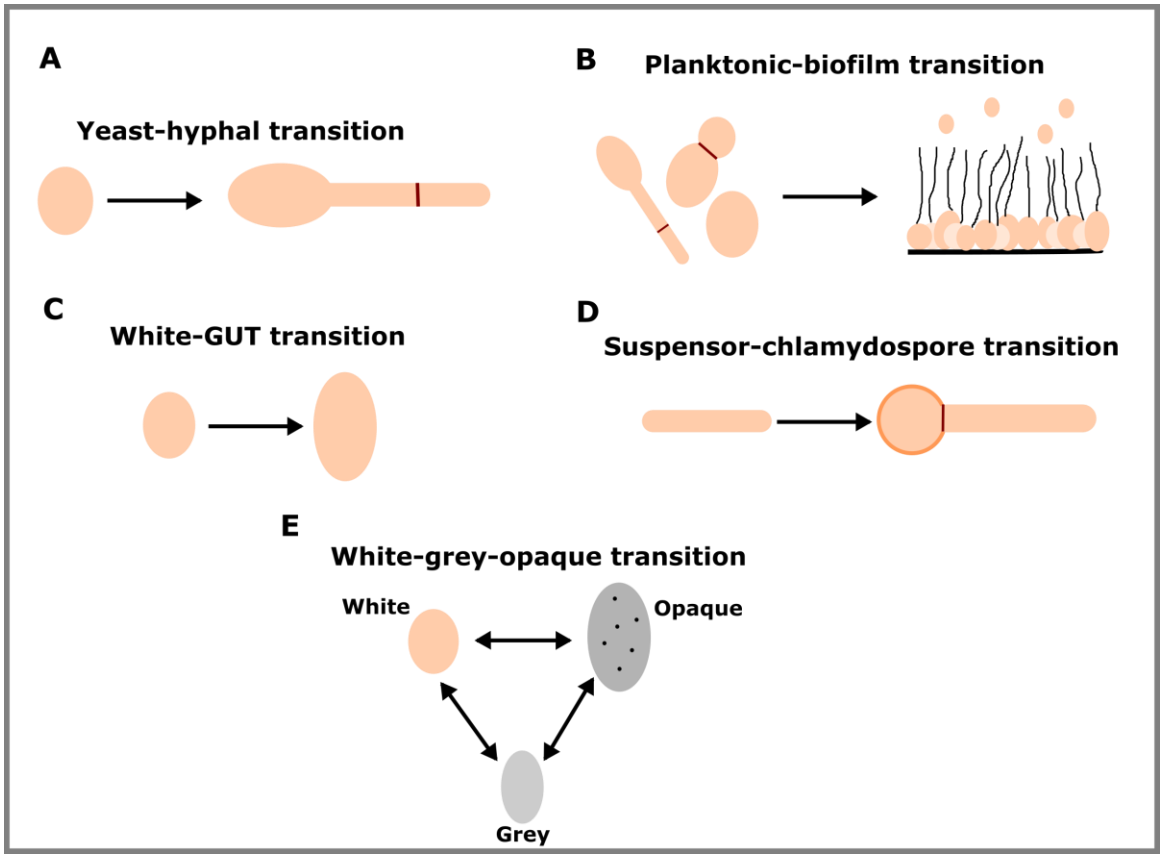


**Figure 3 Different morphological transitions in *C. albicans*.**
(A) Yeast-hyphal transition and (B)Planktonic-biofilm transition, are important for pathogenicity of *C. albicans* (C) White-GUT transition, important for commensal lifestyle (PANDE *et al.* 2013). (D)Suspensor-chlamydospore transition, the function is unknown. Suspensor cells are formed from filamentous cells but differ from true hyphae in being wider (WHITEWAY AND BACHEWICH 2007). (E) White-grey-opaque transition, crucial for mating (MILLER AND JOHNSON 2002; TAO *et al.* 2014).

### 1.4.1 Yeast-hyphal transition

Filamentous (pseudohyphae and hyphae) forms of hyphae are intrinsically invasive in nature and were thus, considered pathogenic, whereas yeast was believed to be associated with the commensal state. However, it has been shown that mutants trapped in either yeast state or filaments were avirulent (MURAD *et al.* 2001; LU *et al.* 2014). This suggests that yeast-to-hyphae transition that is the ability to interconvert between yeast and hyphae is a virulence factor. Also, recent studies suggest that both yeast and hyphal forms coexist as commensal. However, hyphal cells might secrete aspartyl proteases to trigger an immune response in the host when it crosses a threshold resulting in the expression of pathogenic traits (WITCHLEY *et al.* 2019).

The yeast-to-hypha transition is triggered by different environmental cues that reflect the host environment, such as nutrient starvation, N-acetyl glucosamine (GlcNAc), serum, $CO_2$ levels, neutral pH, temperature, and surface contact (BASSO *et al.* 2018). These cues lead to the activation of several downstream pathways that activate transcriptional regulatory circuits. The serum is the most widely used inducer in laboratory conditions. However, its complex composition makes it difficult to identify the factor responsible for filamentation. GlcNAc containing media and Spider medium are also used for inducing morphogenesis *in vitro.* Filamentation is favored at slightly neutral to alkaline pH. However, yeast form is predominant at acidic pH. High temperature promotes filamentation via molecular chaperones Hsp90 and transcription factor Sfl2. **Figure 4** summarizes signal transduction pathways and regulatory networks of yeast-hyphal transition.

Different inducers have only moderately overlapping genetic requirements; most of these are condition-specific. Additionally, solid and liquid filamentation also lead to activation of distinct genetic circuits. Despite these variances, comparative analysis has suggested a common core network of filamentation which is independent of induction conditions. A set of 144 genes is shown to be differentially regulated in both liquid conditions and solid condition. One plausible reason for such an organization could be that all the stress inducers converge at a common phenotypic solution which is filamentation. Also, it is possible that since *C. albicans* reside in diverse niches within the human body, different filamentation programs ensure its survival *in vivo (AZADMANESH et al. 2017).*

### 1.4.2 Planktonic-biofilm transition

*C. albicans* can also exist as biofilms, which are 3D communities of free-floating cells (yeast, pseudohyphae, and hyphae) that adhere to a solid surface and are encased in thick extracellular matrix. The free-floating forms are collectively referred to as planktonic. Biofilms are readily formed on medical devices including catheters, pacemakers, prosthetics, and dentures. They are resistant to most antifungals, host-immune system and other environmental perturbations making biofilm-based infections a significant challenge in clinics. Thick extracellular matrix makes *C. albicans* biofilms impermeable to most antifungals. Moreover, the upregulated expression of efflux pumps and the presence of persistor cells with decreased metabolic activity contribute to antifungal resistance (LOHSE *et al.* 2018).

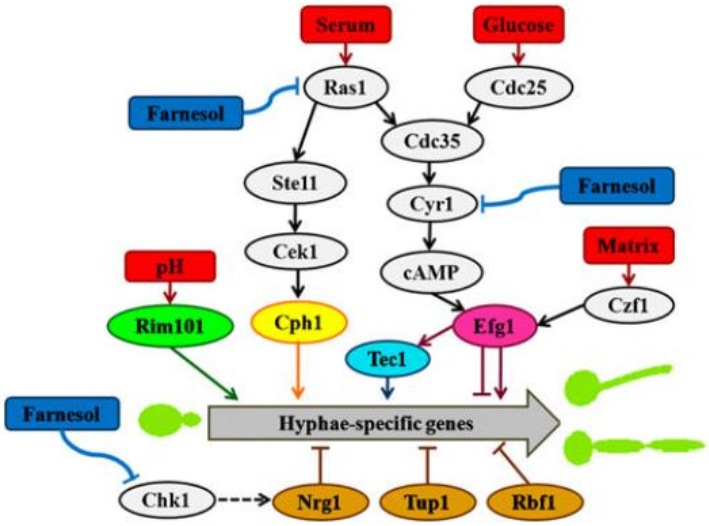


**Figure 4 Signal transduction pathways regulating yeast-hyphal transition.**
Environmental factors such as pH, serum, glucose, and a matrix induce switching from the yeast form to filamentous forms. Alkaline pH is sensed by the RIM101 pathway that proteolytically activates *Rim101* transcription factor which in turn lead to activation of Hyphal-Specific Gene expression (HSGs) and filamentation. *Cph1*, *Efg1*, and *Tec1* are positive regulators. Interestingly, *Efg1* act as an activator of yeast-hyphae transition under normoxia. However, in hypoxia, it acts as a repressor of hyphal growth on agar. The *Nrg1-Rpg1-Tup1* pathway and the *Rbf1* pathway are two negative regulatory pathways that inhibit yeast–filament switching. [Image reproduced from (LIM *et al.* 2012)]

Biofilm formation is divided into four distinct steps: adherence, initiation, maturation, and dispersion. It begins with adherence of yeast cells to a solid surface. Subsequently, pseudohyphal and hyphal cells start appearing which further matures to give thicker biofilms. Once fully matured yeast cells bud of from hyphal cells, they are referred to as dispersed yeast cells. They differ from planktonic yeast cells as they express enhanced virulence-associated characteristics and drug resistance. The mRNA profile of dispersed yeast cells reveals that they are developmentally distinct from both biofilm and planktonic yeast cells (UPPULURI *et al.* 2018). Hence, they can readily move to an alternate site and initiate new biofilm formation (NOBILE AND JOHNSON 2015).

More than 50 transcriptional regulators have been linked to *C. albicans* biofilms. Genetic screens performed with deletion mutants of *C. albicans* identified a core set of nine regulators (**Figure 5**). These regulators are important for both *in vitro* and *in vivo* biofilm models (NOBILE AND MITCHELL 2005; NOBILE *et al.* 2012; FOX *et al.* 2015). Biofilm circuit comprises about 15% of the genome. Interestingly, an evolutionary analysis performed on them revealed that biofilm formation is a more recent phenomenon (NOBILE *et al.* 2012). Most of the genes in the biofilm circuit are relatively new and have undefined roles.

Moreover, temporal regulation of biofilms is still not fully understood, particularly it would be interesting to find how planktonic cells advance to form biofilms. There are studies where gene expression at different time points (8h, 24h, and 48h) of biofilm formation have been checked. However, such studies fail to give a complete picture as gene expression is a dynamic process and each cell behave differently.

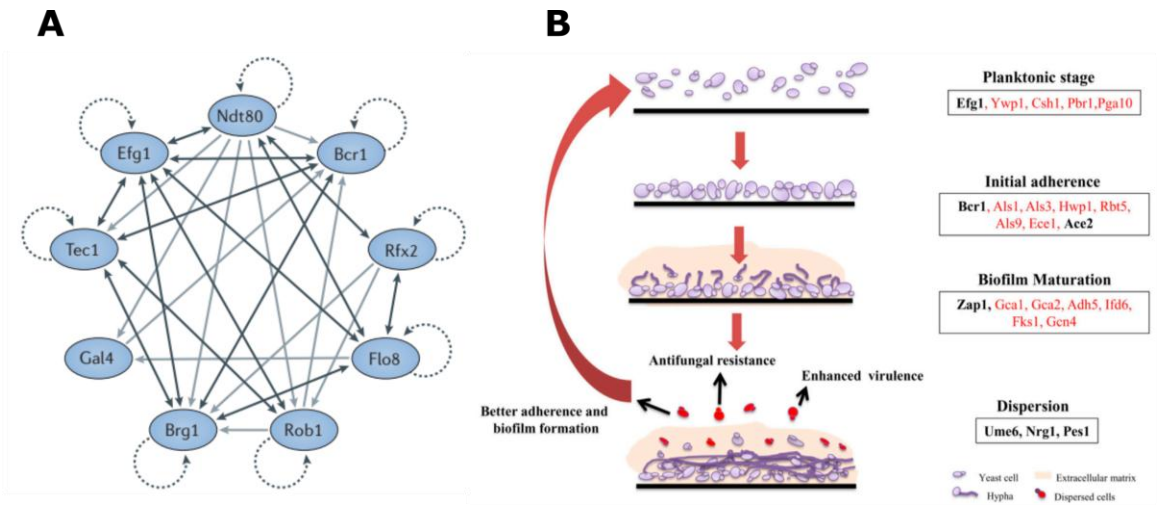


**Figure 5 The core transcriptional network controlling biofilm formation in *Candida albicans*.**
(A) A core set of nine transcriptional regulators are required for biofilm formation. These regulators control the activity of each other indicated by double-headed dark grey arrows and single headed light grey arrows. Moreover, they have autoregulatory activity indicated by dotted arrows. [Image reproduced from (LOHSE *et al.* 2018)].
(B) Development phases of biofilm. Important genes involved in each step is mentioned. Genes written in bold are transcription factors. Image reproduced from [(ALIM *et al.* 2018)]

## 1.5 H3V$^{CTG}$: Negative regulator of planktonic-biofilm transition

H3V$^{CTG}$ is a novel histone H3 variant that is conserved in the CTG clade of ascomycetes including *C. albicans (RAI 2014)*. Previous work done in the lab suggested that H3V$^{CTG}$ (*hht1/hht1*) null cells produce thicker and more robust biofilms as compared to wild type **(Figure 6)**. Also, *hht1Δ* cells exhibit hyperfilamentation in solid media however, there is no effect on liquid filamentation. Hence, H3V$^{CTG}$ negatively regulates planktonic-biofilm transition without affecting yeast to hyphal transition in liquid media. Moreover, it has been shown that H3V$^{CTG}$ occupancy at the promoters of biofilm relevant genes is higher in planktonic condition as compared to biofilm whereas canonical histone H3 occupancy remains unaltered. This further indicates that H3V$^{CTG}$ inhibit expression of biofilm relevant

genes. Furthermore, deletion of H3V$^{CTG}$ could rescue the biofilm defect associated with deletion of master regulators, Bcr1, Tec1, and Ndt80.

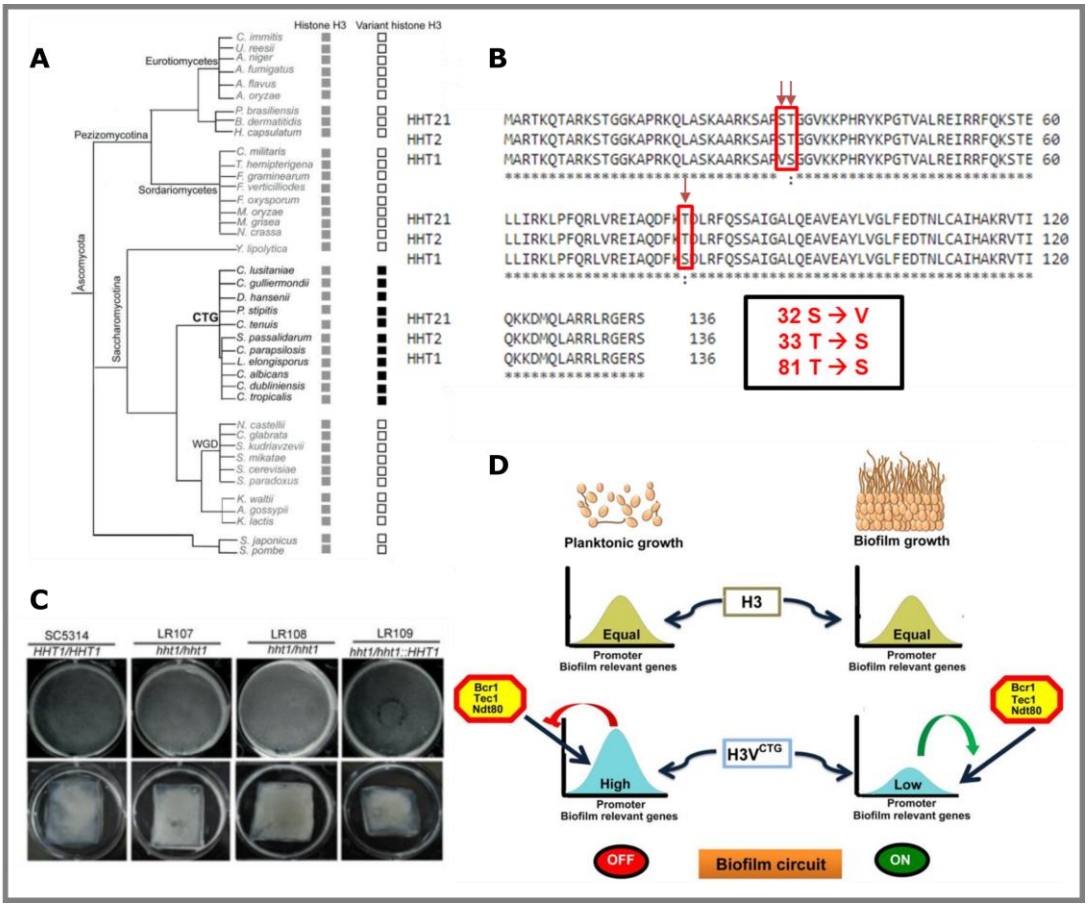


**Figure 6 H3V$^{CTG}$ negatively regulate planktonic to biofilm transition**
(A) Phylogeny showing conservation of H3V$^{CTG}$ in CTG clade of Ascomycota. Canonical histone H3 (grey box) along with presence (black box) or absence (empty box) of variant histone H3 is shown. (B) Amino acid sequence alignment of canonical histones (*HHT2* and *HHT21*) and variant histones (*HHT1*). Red boxes indicate a difference in the sequence. (C) Biofilms were grown on 6-well polystyrene plates (top panel) and silicone sheets (bottom panel). Wild type (SC5314) showed less robust biofilm formation as compared to *hht1Δ* (*hht1/hht1)* and the reintegrant strain (*hht1/hht1::HHT1*). (D) Schematic showing reduced levels of H3V$^{CTG}$ at promoters of biofilm relevant genes in biofilm conditions. This reduced occupancy enables expression of biofilm-relevant genes.

## 1.6 Objectives and rationale of the study

Earlier studies have demonstrated that induction of hyphal growth is interconnected with the expression of hyphal-specific genes (HSG) (BISWAS *et al.* 2007; SUDBERY 2011; WANG AND FRIES 2011). However, this was proved wrong in a study wherein it was shown that upon deletion of genes required for metabolizing a hyphal inducer, GlcNAc, *C. albicans* was able to grow hyphae. Surprisingly, this yeast-hyphal transition was not coupled with the concomitant expression of hyphal-specific genes (NASEEM *et al.* 2015). This suggests that

hyphal morphogenesis and associated gene expression can be regulated independently. It is further supported by the differential ability of hyphal inducers to stimulate hyphal-specific gene expression (MARTIN *et al.* 2013). Moreover, it has been shown that even in the absence of critical transcriptional regulators of HSG expression, Efg1, and Cph1, hyphae formation can be triggered on the surface of the tongue or in matrix-embedded conditions (RIGGLE *et al.* 1999). This substantiates that hyphal growth and HSG gene expression are independent of each other. In the current study, we aimed to find novel and unique regulators of morphogenesis and HSG expression. Our approach towards this was to develop a *C. albicans* whole-cell biosensor which can enable us to determine the expression of hyphal-specific and yeast-specific genes under different conditions in real time. Preliminary results pertaining to this will be discussed in this thesis.

Yeast to hyphal transition plays an important role in the pathogenesis of *C. albicans.* However, its role during commensal growth was not established until recently (DESAI AND LIONAKIS 2019; WITCHLEY *et al.* 2019). A group of scientists has shown that yeast to hyphal transition has an inhibitory role during commensal growth. Moreover, they have proved that limiting commensal fitness occurs independently of fungal morphology (hyphal growth) and is rather dependent on hyphal-specific gene expression. Surprisingly, the authors also observed that *Ume6* deletion mutants were able to form hyphae *in vivo* which otherwise fail to form hyphae in laboratory conditions. This emphasizes that the *in vivo* scenario could be very different from *in vitro* conditions. Hence, we aim to probe this difference by using microfluidics wherein we will use our whole-cell biosensor strain to trace the temporal progression of biofilm development under constant flow and temperature. Such a condition mimic *in vivo* situation and hence would be more informative.

In addition to the above objectives, I have also been working on the factors that regulate planktonic to biofilm growth transition. $H3V^{CTG}$ have been shown to negatively regulate planktonic-biofilm transition. However, the exact mechanism remains to be determined. We believe that variant histone H3 regulates this process by uniquely interacting with a set of other proteins. Keeping this in mind, we are performing an immunoprecipitation experiment with $H3V^{CTG}$ to find its interactome.

# 2. RESULTS

## Part I: Biosensor strain for yeast-hyphal transition

To study yeast-hyphal transition and its association with hyphal-specific gene expression, we aimed to develop a whole-cell biosensor strain of *C. albicans* where both the regulative region (promoter) and the reporter protein would play a vital role. Promoter regulated the expression of the reporter protein in a specific condition will provide a signal that can be interpreted qualitatively or quantitatively (BEREZA-MALCOLM *et al.* 2014). For this purpose, we tagged promoters of a yeast-specific (*NRG1*) and hyphal-specific (*BRG1*) gene with fluorescent markers in *C. albicans* SN148 background. Nrg1 act as a negative regulator (MURAD *et al.* 2001) and Brg1 act as a positive regulator (HOMANN *et al.* 2009) of yeast-hyphal transition. This is further supported by RNA-Seq data *(GRUMAZ et al. 2013)*.

### 2.1 Filamentation of *URA3* auxotrophic strains in the presence of galactose

*URA3* is critical for morphogenesis and virulence of *C. albicans* (LAY *et al.* 1998; BAIN *et al.* 2001). We also observed that unlike SN148 $Ura^+$ strain, isogenic $Ura^-$ derivatives failed to transit in hyphal forms in the presence of commonly used hyphal-inducing conditions (YPD + 10% serum or YPD + 10mM GlcNAc). However, on increasing the signal strength by using 20% serum, filamentation could be observed. Also, replacing glucose in YPD with galactose led to filamentation in the presence of 10mM GlcNAc. This is because glucose causes downregulation of GlcNAc transporter, *NGT1* thus preventing its uptake (ALVAREZ AND KONOPKA 2007; GUNASEKERA *et al.* 2010). GlcNAc induction has advantages over conventional inducing conditions. It enables hyphal growth over a prolonged period without significant reversion to yeast growth form and with high biomass yields (HEILMANN *et al.* 2011). Moreover, in this condition, hyphal cells aggregate less thus facilitating downstream applications such as microscopy (**Figure 7**).

### 2.2 Nrg1 expression increases and Brg1 expression decreases during yeast-hyphal transition

To construct the biosensor strain, we expressed GFP from the *NRG1* promoter and mCherry from the *BRG1* promoter using *HIS1* and *ARG4* as selectable markers respectively in *C. albicans* SN148 ($Arg^-$, $Leu^-$, $His^-$, $Ura^-$).

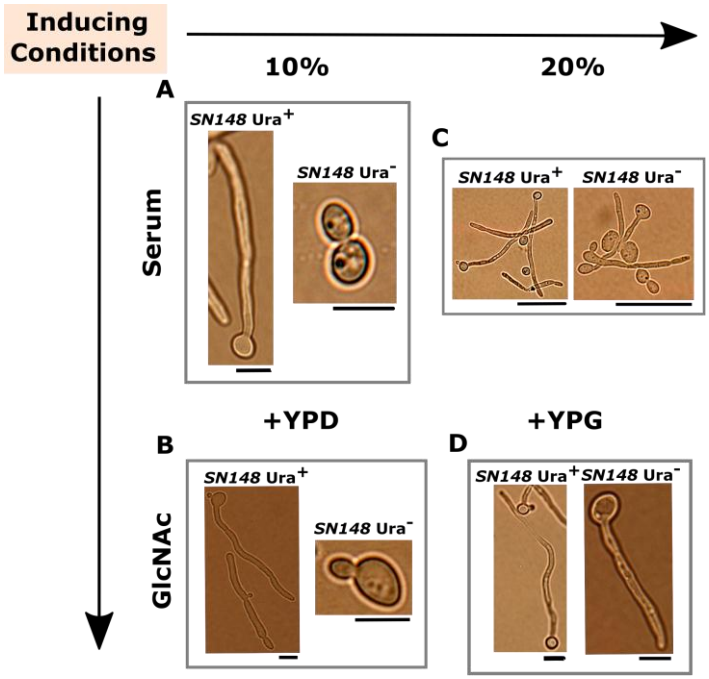


**Figure 7 Filamentation of *URA3* auxotrophs in response to different inducing conditions.** Filamentation of SN148 Ura$^+$ and Ura$^-$ strains were performed to find a suitable induction condition for the biosensor strain (His$^+$, Arg$^+$, NAT$^+$, Ura$^-$ and Leu$^-$). (A) and (B) Ura$^-$ strain failed to filament at 37°C in response to YPD + 10% serum and YPD + 10mM GlcNAc. (C) and (D) Ura$^-$ strain filamented at 37°C in response to YPD + 20% serum and YPG + 10mM GlcNAc. Replacement of glucose carbon source to galactose led to morphogenesis with lesser aggregation and more sustained hyphal growth.

We analyzed the biosensor strain by microscopy, and we observed that GFP expression driven by *NRG1pr* decreased and mCherry expression driven by *BRG1pr* increased as *C. albicans* cells switch from yeast to hyphal state. A sharp increase in mCherry signal was observed at 3h. However, a slow trend of reduction in GFP fluorescence is distinguished due to the long half-life of GFP and the dilution effect of successive generations of yeast (**Figure 8**, **Figure** 9).

Live-cell microscopy was performed to further validate the biosensor strains (**Figure 9**). Upon induction, GFP expression decreased whereas mCherry expression increased. However, hyphal formation was relatively slower on an agarose pad. Most cells after 3h were pseudohyphal in nature. This could be because hyphal formation occurs at 37°C whereas pseudohyphae forms at 35°C (SUDBERY 2001). It suggests that probably temperature was not accurately maintained at 37°C while performing live-cell imaging.

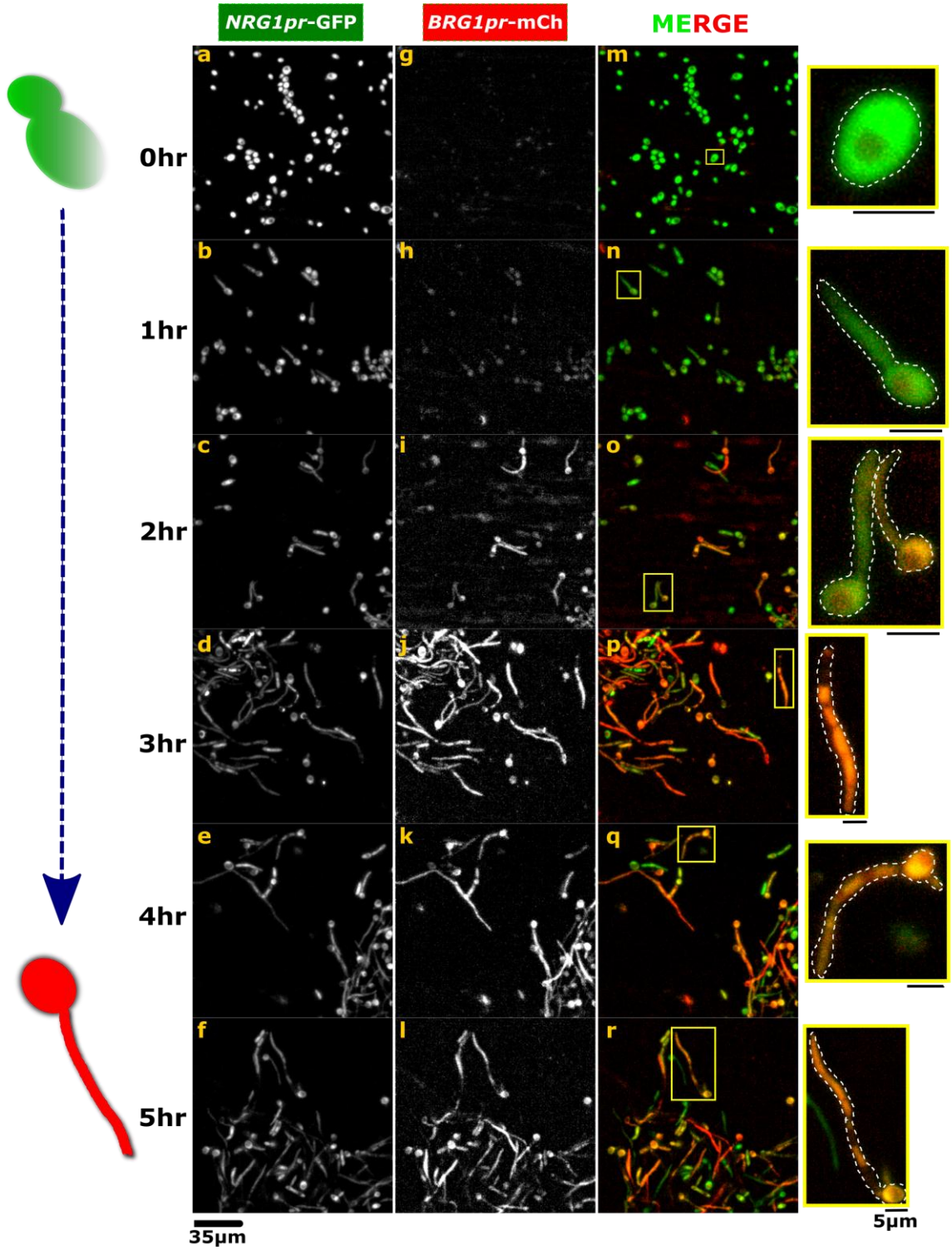


**Figure 8 Kinetics of Nrg1 and Brg1 expression during the yeast-hyphal transition.**
(a)-(f) Time course study of *Nrg1pr* expression during the yeast-hyphal transition. (g)-(l) Time course study of *Brg1pr* expression during the yeast-hyphal transition. (m)-(r) Merged images. Zoomed in images of (m)-(r) are shown in the extreme right panel. Time points taken 0-5h.

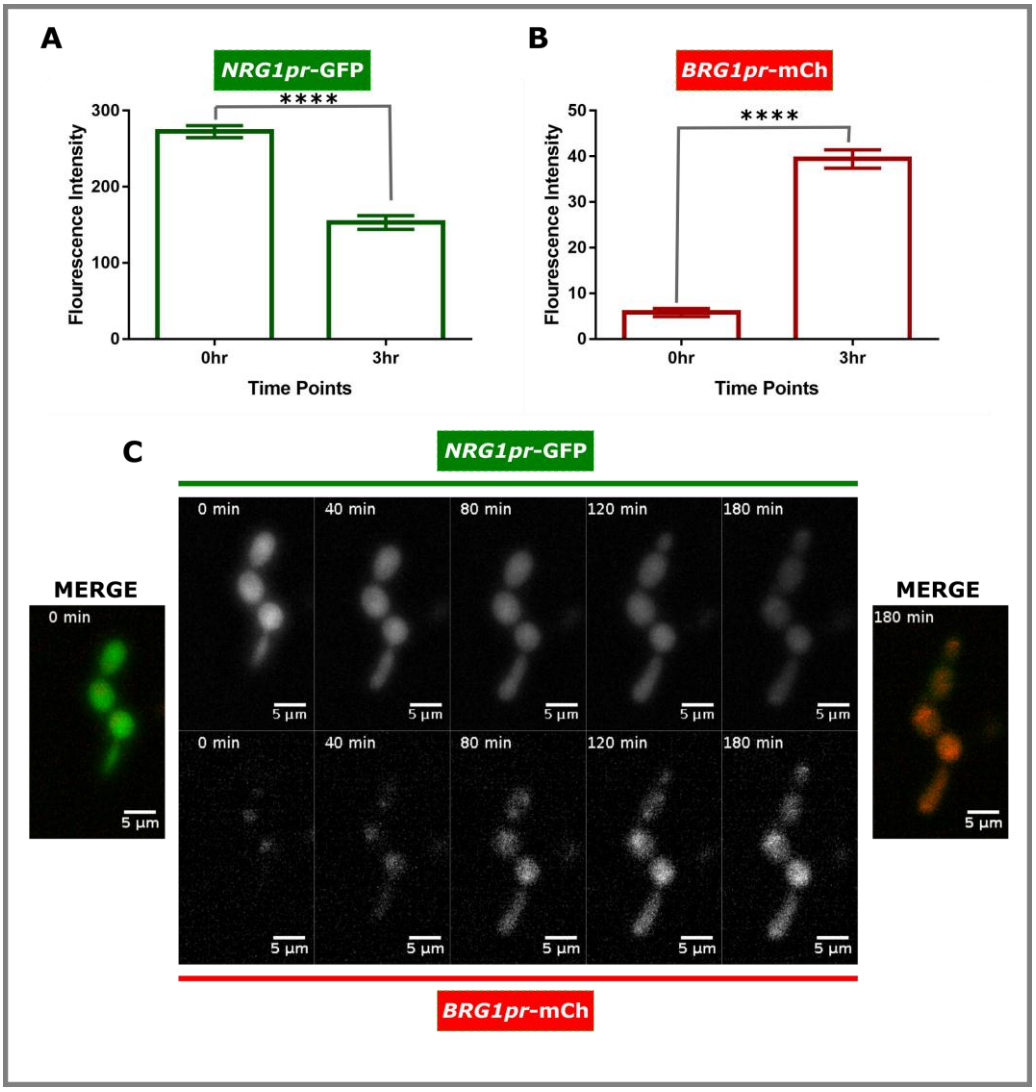


**Figure 9 Change in intensity of fluorescence markers during the yeast-hyphal transition.** Quantification of fluorescence intensity of *NRG1pr*(A) and *BRG1pr*(B) during the yeast-hyphal transition. GFP fluorescence decreased whereas mCherry increased at 3h. P<0.0001, unpaired t-test. (B) Live-cell microscopy. GFP expression was completely taken over by mCherry as indicated by the merged images of 0 min and 180 min (extreme left and right). GFP panel (top) showed a decreasing fluorescence and mcherry panel (bottom) indicated an increasing fluorescence.

## Part II: Novel regulators of planktonic-biofilm transition

Our knowledge about the soluble complexes formed by H3V$^{CTG}$ from planktonic to biofilm state is limited. Considering its essential role in negatively regulating biofilm formation we expect that an immunoprecipitation experiment with H3V$^{CTG}$ can give us useful insights about the regulation of this switch. We might identify novel regulators of this transition. Moreover, we speculate that H3V$^{CTG}$ could be uniquely interacting with specific chromatin-remodelers that enable its eviction in biofilm state. Hence, to find the interactome of H3V$^{CTG}$ we tagged it with V5 epitope. Further, we have validated that the tagged protein is functional by a phenotypic assay.

### 2.3 Both copy tagging of H3V$^{CTG}$ with V5 epitope is functional

C-term of H3V$^{CTG}$ was tagged with V5 epitope to enable an immunoprecipitation experiment for determining its interactome in specific conditions. We tagged one copy of *HHT1* in *C. albicans* SC5314 background to check the expression of epitope-tagged H3V$^{CTG}$. Western analysis confirmed that the tag was being expressed (**Figure 10A, B**). Furthermore, *HHT1* was tagged with V5 in a strain where one copy of the gene is deleted (LR105) to check the functionality of epitope-tagged H3V$^{CTG}$.

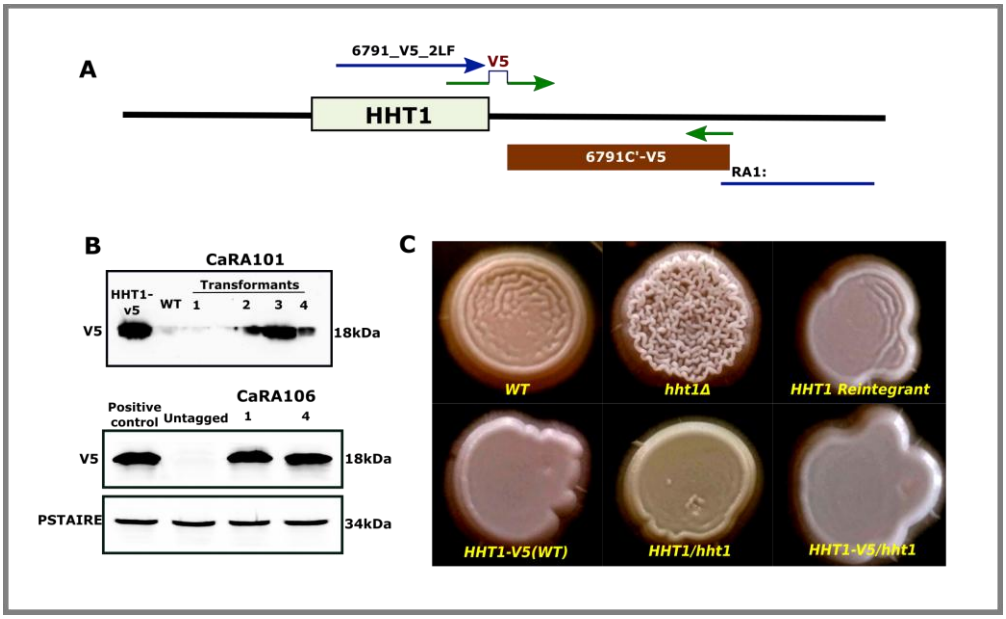


**Figure 10 H3V$^{CTG}$ tagged with V5 epitope is functional.**
(A) Line diagram is depicting C-term tagging of *HHT1*. (B) Western blot analysis using V5 antibodies confirmed expression of H3V$^{CTG}$-V5 (18kDa) in CaRA101 (*HHT1-V5/HHT1*) and CaRA106 (*HHT1-V5/hht1*). (C) Spotting assays revealed WT (wild-type), *HHT1* reintegrant (LR115) and *HHT1/hht1* (LR105) have smooth colony morphology whereas *hht1Δ* (LR107) have wrinkled colony morphology. Like WT, CaRA106 (*HHT1-V5/hht1*) also had smooth colony morphology indicating that the tagged copy of *HHT1* is functional.

Deletion of *HHT1* leads to a wrinkled colony morphology in spider media due to hyperfilamentous nature (**Figure 10C**). Reintegration of *HHT1* in *hht1/hht1* rescues the phenotype hence suggesting that the filamentous phenotype was indeed due to the absence of *HHT1*. CaRA106 (*HHT1-V5/hht1*) did not show wrinkled colony morphology thus indicating that the V5 tagged $H3V^{CTG}$ is functional. Next, both the copy of *HHT1* was tagged with V5 in LR144 (*HHT1/HHT1-V5-HIS1*). Integration was confirmed by Southern and spotting assay revealed that both the copy tagged strain of *HHT1* is functional (**Figure 11**).

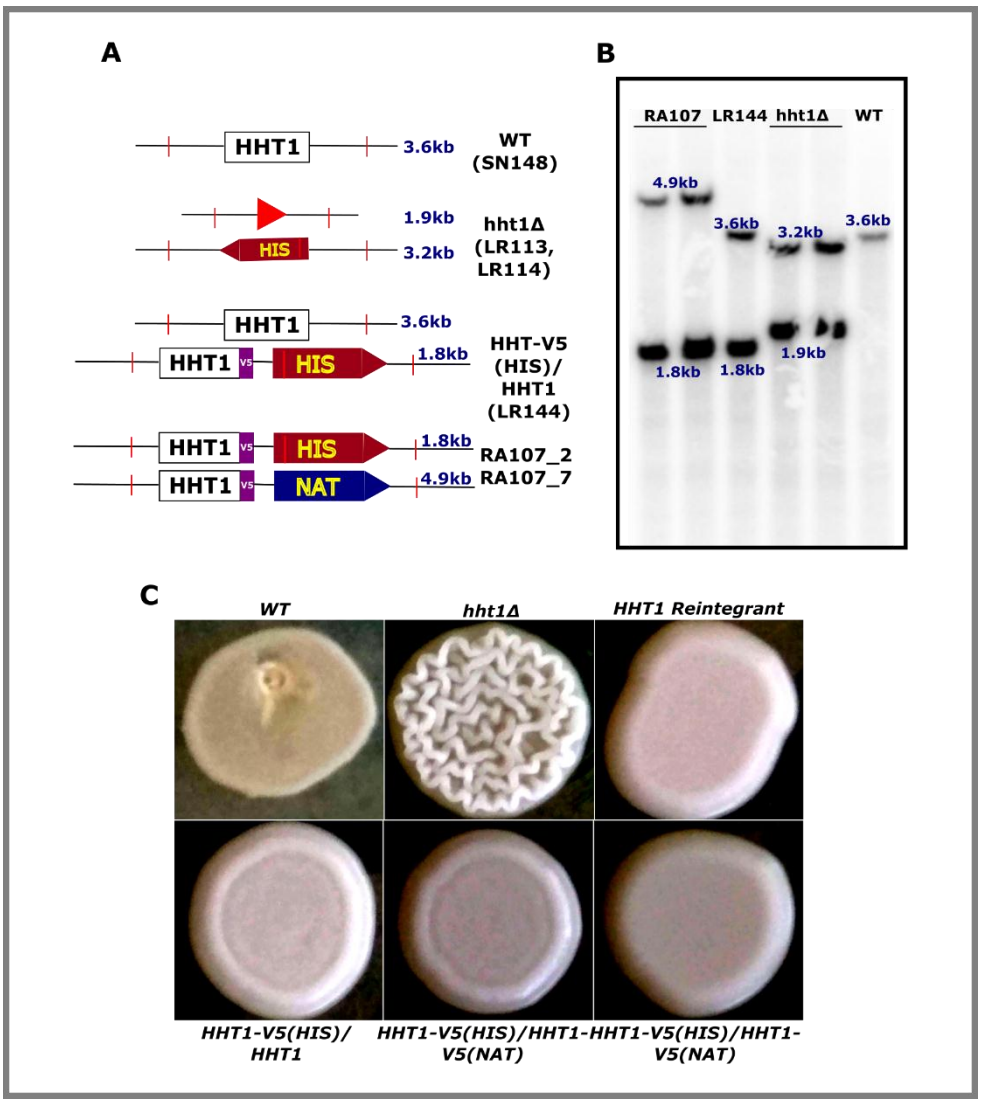


**Figure 11 *HHT1* both copy tagged strain is functional.**
(A) Southern blotting was performed to confirm correct integration. Red bars indicate NcoI enzyme site. (B) The expected pattern was observed after Southern hybridization. (C) Spotting assays revealed that CaRA107 (*HHT1-V5-NAT/HHT1-V5-HIS1*) strains express functional $H3V^{CTG}$. Hence the strain can be used to perform mChIP.

## 2.4 Immunoprecipitation of H3V$^{CTG}$ using V5 antibody

Immunoprecipitation was performed using a previously described mChIP protocol to find the interacting proteins of H3V$^{CTG}$ (JI *et al.* 2015; WIERER AND MANN 2016), (**Figure 12A)**. We compared both the physical method (sonication $^{S}$) and the enzymatic method (DNase $^{D}$). DNase treatment resulted in a fragment size of 200-700bp (**Figure 12B**). Moreover, there was a significant loss of protein in the pellet fraction after both sonication and DNase treatment as revealed after Coomassie staining (**Figure 12C**). Bands for some interacting proteins along with H3V$^{CTG}$ could be observed on the silver stained gel (**Figure 12D**). Immuno-pull down with sonicated sample worked with better efficiency than DNase treated sample.

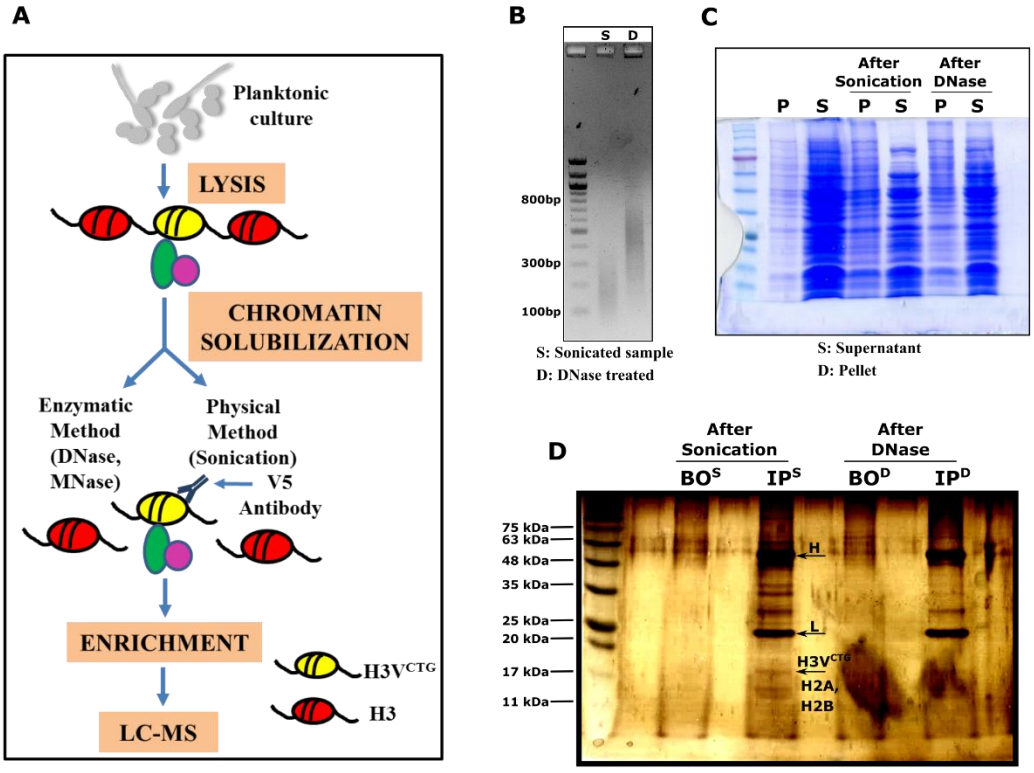


**Figure 12 Immuno-precipitation of H3V$^{CTG}$ using V5 antibody.**
(A) Schematic representing the workflow of H3V$^{CTG}$ mChIP. (B) Fragment sizes obtained after sonication(S) and DNase(D). (C) Coomassie staining depicting significant loss of protein in the pellet(P) fraction both after sonication and DNase treatment. (D) Silver staining of immunoprecipitated sample. BO- Bead only control, IP- immunoprecipitated sample.

# 3. DISCUSSION

In this work, we attempted to develop a mechanistic understanding of the morphogenesis process in fungal species. *C. albicans* is the most commonly isolated organism in clinical settings and is the most successful opportunistic pathogen due to several hallmark features of its biology (LEGRAND *et al.* 2019). Moreover, it exhibits remarkable phenotypic plasticity which is closely associated with the virulence potential of the organism. This prompted us to perform our studies in *C. albicans.*

*C. albicans*, being polymorphic in nature, undergoes several growth-phase transitions including yeast-hyphal, planktonic-biofilm, and white-opaque transition. Considering, the importance of yeast, filamentous (hyphae and pseudohyphae) and biofilm structures in the pathogenesis of the organism, we focused on yeast-hyphal and planktonic-biofilm transitions. Both yeast and hyphal forms are present in the commensal as well as the pathogenic lifestyle of the organism (WITCHLEY *et al.* 2019). Hyphal cells are crucial for the pathogenesis of the organism as it invades and damages the tissues. Hyphal growth is generally coupled with the expression of hyphal-specific genes (HSG) such as adhesins and several proteases which are vital for virulence (LANE *et al.* 2001; GOW *et al.* 2002; CARLISLE *et al.* 2009; MOYES *et al.* 2016; NOBLE *et al.* 2017). Recent studies suggest that hyphal growth and HSG expression can be independent of each other(NASEEM *et al.* 2015). Yeast cells can also express hyphal-specific (virulence-associated) genes. For example, dispersed yeast cells from mature biofilms express genes important for adhesion and filamentation (UPPULURI *et al.* 2018). Both yeast and filamentous forms are important for virulence and ability to switch between the two is an important virulence factor.

Our approach towards gaining more insights into the molecular process of morphological switching was to develop a fluorescence-based *C. albicans* whole-cell biosensor (**Figure 13**). The strain was designed to enable the study of this transition qualitatively and quantitively in real time. We tagged a yeast-specific gene with GFP as a marker and a hyphal-specific gene with mCherry as the marker. On exposure to hyphal-inducing conditions, yeast cells formed germ tubes and further mature hyphae. GFP expression in the yeast state was completely taken over by the increasing mCherry expression in the hyphal state. This suggests an association between hyphal growth and hyphal-specific gene expression in the condition tested. However, due to the long half-life of GFP, drop in GFP expression was not as distinguished. Hence, our sensor gives a higher resolution for mCherry induction patterns than for GFP repression.

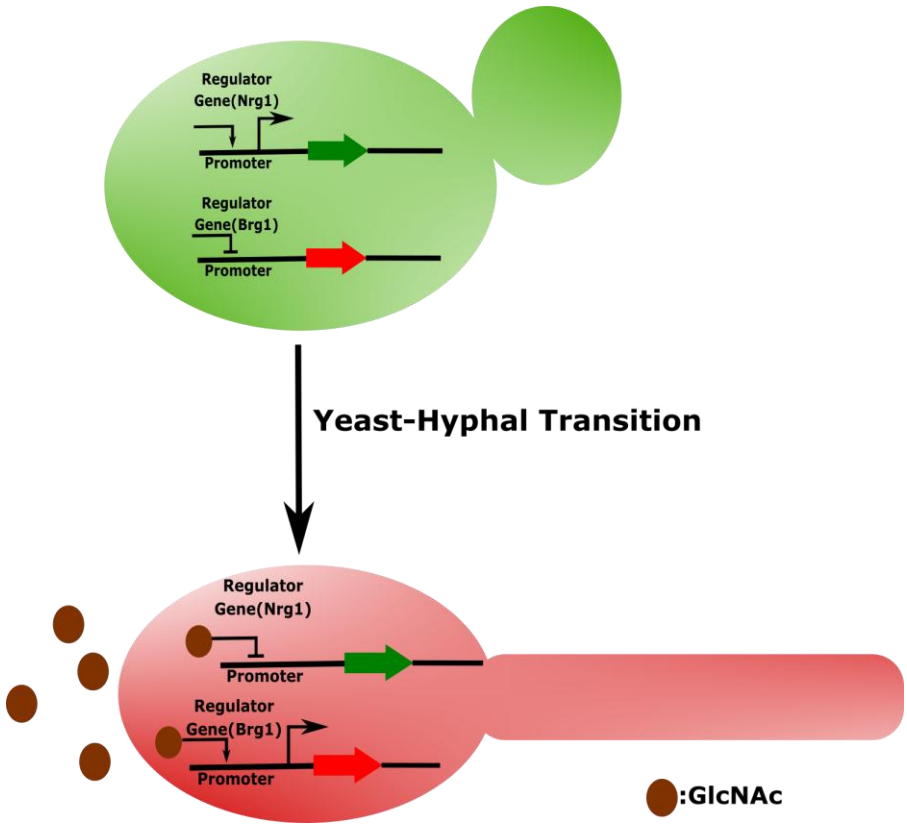


**Figure 13 Diagrammatic representation of transition of GFP expressing yeast cell into mCherry expressing hyphal cell.**
In the presence of hyphal-inducing conditions (10mM GlcNAc), GFP expressing yeast cell transit into mCherry expressing hyphal cell.

The biosensor strain offers several advantages and can be used to test the effect of different gene mutations on both hyphal architecture and hyphal-specific gene expression. It would enable flow cytometry analysis which is inexpensive and less time-consuming than microscopy since a large number of cells can be analyzed in a short time (BLEICHRODT AND READ 2018). However, for experiments that require prolonged filamentation, microscopy can be used. The biosensor can also be used as a marker inside live infected animals thus enabling *in vivo* studies.

Next, we aimed to find the interactome of $H3V^{CTG}$, a novel histone H3 variant that acts as a negative regulator of planktonic-biofilm transition (RAI 2014). Intricate knowledge of protein-protein interaction aid in the understanding of gene regulation and other chromatin-related processes. Analysis of H3.1 interactome provided a comprehensive view of associated chaperones and components of the replication fork (CAMPOS *et al.* 2015). Therefore, we planned to perform an immunoprecipitation experiment and high throughput mass spectrometry analysis using our $H3V^{CTG}$. In this study, we tagged $H3V^{CTG}$ with V5

epitope. Moreover, we have shown that the tagged protein is functional using spotting assays. We are currently performing immuno-pull down using a mChIP (modified Chromatin Immunoprecipitation) method. Conventional methods of immunoprecipitation could not be used since histones are tightly associated with chromatin and thus require an additional step for chromatin solubilization. Therefore, we tried to standardize immune-pull down using the mChIP method.

# 4. FUTURE PERSPECTIVES

*C. albicans* virulence is closely associated with the expression of hyphal-specific genes. Interestingly, expression of hyphal-specific genes may not always be associated with hyphal growth in all conditions. Hence, hyphal growth can be dependent as well as independent of transcriptional regulation. Such genes which are uniquely essential for virulence and not hyphal architecture can be potent antifungal targets. We plan to use our biosensor strain to find such novel targets for antifungals. For this purpose, we plan to screen an overexpression library of *C. albicans* genome (CHAUVEL *et al.* 2012). Approximately 6000 ORFs are cloned under an inducible-tetracycline promoter which enables the overexpression of the gene. We would start with a yeast-locked strain that would be expressing GFP ($GFP^+$). GFP fluorescence signifies yeast-specific gene (YSG) whereas mCherry fluorescence signifies hyphal-specific gene (HSG) expression. The yeast-locked strain will be transformed with a cocktail of all the cassettes in the library. Upon induction of over-expression with doxycycline, we expect two major populations: $GFP^+$ yeast cell (Yeast-specific Gene expression, YSG) and $mCherry^+$ hyphal cell (Hyphal-specific Gene expression, HSG). However, we expect two more populations: $GFP^+$ hyphal cell and $mCherry^+$ yeast cell. Overexpression of some genes might lead to activation of hyphal-specific gene expression in a yeast cell. Hence, this would enable us to find genes that might be essential for virulence but not hyphal architecture. Characterization of such genes can be performed by flow cytometry and will be particularly interesting as they can serve as better targets for antifungals.

Moreover, we plan to use this strain for understanding the effect of geometric constraints on morphogenesis. Several studies from G.V. Shivashankar's group have highlighted that geometric constraints lead to changes in gene expression profiles and differentiation programs (JAIN *et al.* 2013; SHAO *et al.* 2015; MAKHIJA *et al.* 2016). We aim to validate the same in *C. albicans* using microfluidics. Microfluidics involves a microfluidic device that has channels where the cells are seeded. These cells are kept in a constant flow of media and a given temperature to allow their growth. The microfluidic device is kept under a microscope which enables the study of growth patterns in real time. For our experiment, we plan to design channels such that they can fit hyphal cells but not yeast cells. Considering previous studies, we expect that when a yeast cell is pushed in the channel, it will undergo morphogenesis. RNA-seq analysis of such yeast cells forced to switch to hyphal form by mechanical signal might reveal a different pattern of gene expression.

Moreover, interactome studies of H3V$^{CTG}$ might reveal novel targets for antifungals that can specifically target biofilms. This will help us to decipher the mechanism by which occupancy of H3V$^{CTG}$ is reduced at the promoters of biofilm-relevant genes as cells transit from planktonic-biofilm conditions.

# 5. MATERIALS AND METHODS

## 5.1 Media, Growth Conditions and transformation

*C. albicans* strains were grown at 30°C in YPD medium (1% yeast extract, 2% peptone, 2% dextrose) unless indicated otherwise. For filamentation, YPG (1% yeast extract, 2% peptone, 2% galactose) with 10mM N-acetylglucosamine was used followed by incubation at 37°C. For spotting assays, spider media plates (1% peptone, 1% yeast extract, 1% mannitol, 0.5% NaCl and 0.2% $K_2HPO_4$, 2% agar) were used.

Cells were transformed by the standard lithium acetate method as described previously (GIETZ AND WOODS 2002). Transformants were selected for on SC medium (2% dextrose, 6.7% YNB with ammonium sulfate, and auxotrophic supplements) or on YPD+clonNAT (1% yeast extract, 2% peptone, 2% dextrose and 100µg/ml nourseothricin) for nourseothricin-resistant isolates.

## 5.2 Genomic DNA preparation

10ml culture of *C. albicans* cells was grown overnight in YPD and harvested by centrifugation at 3800 rpm for 5 min. Cells were washed with autoclaved water and resuspended in 200µl extraction buffer. Cells were lysed by vortexing with 0.3g of acid-washed glass beads and 200µl of phenol: chloroform: isoamyl alcohol (25:24:1). Next, 200µl of 1X TE was added to the tubes followed by centrifugation at 13,000 rpm for 10min. The supernatant was collected, and DNA was precipitated by 100% ethanol at -20°C for 1h. The tubes were centrifuged at 13,000 rpm and the pellet obtained was washed with 70% ethanol. The pellet was air-dried and resuspended in 30µl of 1X TE and 1µl RNase A.

## 5.3 Plasmid and Strain Construction

All the plasmids and C. albicans strains used in the study are listed in the **Table 3**. All the primer sequences used are listed in the **Table 5**.

### 5.3.1 Construction of Biosensor strain

A trans-activator cassette, pNIMX (CHAUVEL *et al.* 2012) was integrated in SN148 strain at *ADH1* locus to enable induction of TET-on system of the overexpression cassettes. Transformants were selected using nourseothricin marker. The resultant strain was named CaRA108. Integration was confirmed using PJ 86/PJ 87 primer set.

A 2.8kb upstream region of *NRG1* (C7_04230W_A) was amplified from *C. albicans* (SN148) genomic DNA using RA9/RA10 primer set. It was then cloned as SacI/SpeI fragment immediately upstream of GFP in the pBS-GFP-HIS1 plasmid (CHATTERJEE *et al.*

2016) to obtain pRA04. The plasmid was confirmed by gel shift and restriction analysis. Sph1 linearized pRA04 was transformed in CaRA108 strain to obtain CaRA109 strain. Transformants were selected for histidine prototrophy. Integration was confirmed by PCR amplification using RA15/RA16 primer set **(Figure 14A)**.

A 2.9kb upstream region of *BRG1* (orf19.4056) was amplified from *C. albicans* (SN148) genomic DNA using RA13/RA14 primer set. It was then cloned as SacII/SpeI fragment immediately upstream of mCherry in pFA-mCherry-HIS (from Sundar). SpeI site was destroyed as the vector was digested with SacII/NheI. Ligation was facilitated since SacII and NheI had compatible cohesive ends. The resulting plasmid was named pRA05. The plasmid was confirmed by gel shift and restriction analysis. SpeI linearized pRA05 was transformed in CaRA109 strain. Transformants were selected for arginine prototrophy. Integration was confirmed by PCR amplification using RA17/RA18 primer set **(Figure 14B)**. The resultant strain was named CaRA110.

CaRA110 strain was auxotrophic for URA gene hence delayed filamentation was observed (LAY *et al.* 1998; CHENG *et al.* 2003). To perform live cell imaging, *URA* gene was integrated at the *RPS10* locus of CaRA110 strain using StuI linearized CIp10 plasmid (MURAD *et al.* 2000). Integration was confirmed by PCR amplification using URA3-CIP10 and UP-RPS10 primer pair **(Figure 14C)**. The resultant strain was named CaRA111.

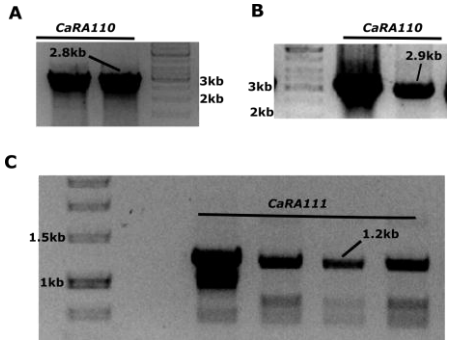


**Figure 14 PCR confirmation of biosensor strain.**
(A) A fragment size of 2.8 kb indicated correct integration of *NRG1pr-GFP* (pRA04) tagging cassette. (B) A fragment size of 2.9 kb indicated correct integration of *BRG1pr-mCherry* (pRA05) tagging cassette. (C) A fragment size of 1.2 kb indicated correct integration of *URA3* at *RPS10* locus.

### 5.3.2 Construction of *HHT1-V5/HHT1 and HHT1-V5/hht1* strains

*HHT1* (C3_07090W_A) C-term was amplified using 6791V5-CFP and 6791V5-CRP primers and cloned in the pBS-NAT vector as SacI/SacII fragment to obtain pRA01 plasmid.

The Ca*HHT1*-V5 cassette was amplified using long primers, 6791V52LFP and RA1. 6791V52LFP had homology to *HHT1* ORF, and RA1 had homology both to NAT and the 3'UTR. The fragment was used to transform *C. albicans* SC5314 strain and transformants were selected for nourseothricin resistance. The resultant strain, CaRA101 was confirmed by PCR. Expression of the fusion protein was confirmed by western blotting using anti-V5 antibody.

To test whether V5 tagged variant histone H3 ($H3V^{CTG}$) is functional or not, *HHT1* was tagged in LR105 strain (*HHT1/hht1*) using pRA01 plasmid. The resultant plasmid was named CaRA106. Expression of the fusion protein was confirmed by western blotting using anti-V5 antibody. Functionality was accessed by spotting assays.

### 5.3.3 Construction of *HHT1-V5-NAT/HHT1-V5-HIS1* strain

Using pRA01 plasmid, the remaining copy of *HHT1* was tagged in LR144 strain (*HHT1/HHT1-V5-HIS1*). Transformants were selected for nourseothricin resistance. The resultant strain, CaRA107 was confirmed both by PCR and Southern hybridization (**Figure 15).**

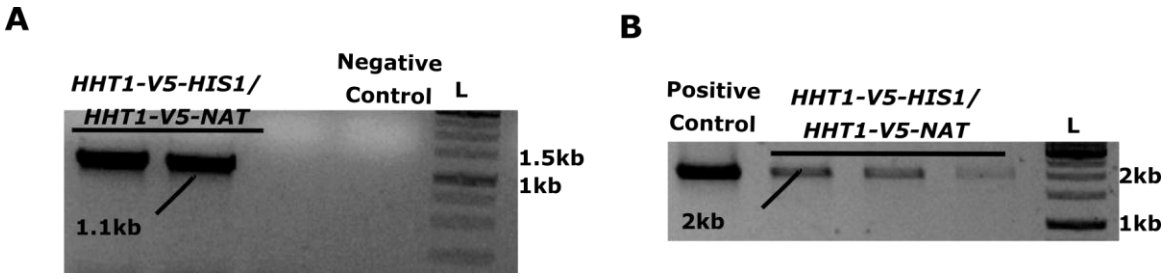


**Figure 15 PCR confirmation of double copy tagged strain.**
(A) A fragment size of 1.1kb confirmed tagging of second copy of *HHT1* using NAT marker. (B) A fragment size of 2kb confirmed tagging of the first copy of *HHT1* using HIS1 marker.

## 5.4 Microscopy and Liquid Filamentation assay

5ml culture of *C. albicans* was grown overnight in YPG (ALVAREZ AND KONOPKA 2007; GUNASEKERA *et al.* 2010). Cells were harvested by centrifugation at 3800 rpm for 5 min. Pellet was resuspended in 5ml of fresh media. Next, 0.2 OD cells were inoculated in hyphal inducing media (YPG + 10mM GlcNAc) followed by incubation at 37°C at 180 rpm. After every subsequent hour, 1ml culture was aliquoted till 5h. The aliquoted culture was pelleted, washed with 1X PBS and stored at 4°C or directly taken for microscopy.

2µl of the cell suspension was placed on a cleaned glass slide and observed at 100X using Zeiss Axio Observer. Images were processed using ImageJ software. For quantification, mean fluorescence intensity of more than 40 cells for each time-point was calculated. Graphs were plotted using GraphPad Prism software. Error bars represent SEM. To compare the mean deviation across two time-points, Student's *T-test* was used.

For live cell imaging, an overnight YPG grown culture was diluted in hyphal inducing media (2% galactose, 10mM GlcNAc, 6.7% YNB with ammonium sulfate, and auxotrophic supplements) and grown for 1h at 37°C and 180 rpm. Next, 2µl of the cell suspension was placed on a slide containing a thin hyphal inducing medium 2% agarose patch and a coverslip was placed on top. Imaging was performed at 37°C at 100X using Zeiss Axio Observer. Images were collected at a 20 min interval. 5% intensity with 100ms exposure time was used for GFP, and 5% intensity with 150ms exposure was used for mCherry. Z-steps were taken at 0.3µm interval. All the images were displayed as maximum intensity projections.

### 5.5 **Western blot analysis**

*C. albicans* strains were grown overnight in YPD and 6 x $10^7$ cells were harvested by centrifugation at 3800 rpm for 5 min. Cells were washed with 1 ml of $dH_2O$ and resuspended in 400µl of 12.5% Trichloroacetic acid (TCA) solution. The cell suspension was frozen at -20°C overnight. Next day, the cells were thawed on ice and pelleted at 13,000 rpm, 4°C for 10 min. The pellet was washed in 80% acetone solution followed by pelleting at 13,000 rpm, 4°C for 10 min. After two rounds of washing, the pellet was air-dried and resuspended in 50µl of lysis buffer (1% SDS + 0.1N NaOH) with 1X loading dye. The lysate was incubated in a boiling water bath for 10 min. Proteins were separated by electrophoresis on a 12% SDS-PAGE gel and blotted onto a nitrocellulose membrane (Amersham Protran Premium, Cat. No. 10600003) in a semi-dry apparatus (Bio-Rad). The blotted membranes were blocked by 5% skim milk containing PBS (pH 7.4) for 30 min at room temperature. The membranes were then incubated with 1:5000 dilution of anti-V5-antibodies (Invitrogen, Cat. No. R6025) or 1:5000 dilution of anti-PSTAIRE antibody (Abcam, Cat. No. ab10345) in 2.5% skim milk in PBS at 4°C overnight with constant shaking. Next, the membrane was washed thrice with PBST (0.1% Tween-20 in 1X PBS) solution. Anti-mouse HRP conjugated antibodies (Bangalore Genei) were added at a dilution of 1:5000 in 2.5% skim milk PBS solution and incubated for 1-2 hr at 4°C on constant shaking. The membranes were then washed thrice with the PBST solution. Signals were detected using the chemiluminescence method.

## 5.6 Southern hybridization

RA107 strains were confirmed using Southern hybridization. Genomic DNA was isolated and quantified using Quantity One software (Bio-Rad). 6-8µg of DNA was digested and separated on an agarose gel. The gel was sequentially treated with 0.25 M HCl for acid nicking of DNA, Denaturation buffer and neutralization buffer. Acid-nicked DNA was transferred by capillary action onto a positively charged nylon membrane (Amersham Hybond-$N^+$, Cat. No. RPN303B) in 10X SSC buffer (Saline-Sodium Citrate). Following transfer, the membrane was washed with 2X SSC, dried and crosslinked by exposure to UV for 5 minutes in Genelinker (Bio-Rad, 12000µJ x 100). The blot was pre-hybridized in 10ml 1x Southern hybridization buffer (10g SDS, 5.8g NaCl, 2.4ml 0.5M EDTA, 20ml 1M sodium phosphate pH7 for 200ml) at 65°C for 2-4hr. The specific probe was radiolabeled with $\alpha^{32}$ P dCTP using a random primer labeling kit (BRIT-LCK-2). 50ng Probe DNA in an appropriate volume of autoclaved water was boiled for 5 min and chilled immediately. Next, 5µl random primer buffer, 5µl random primers, 12µl dNTP cocktail except dCTP, 4µl $\alpha^{32}$ P dCTP and 2µl Klenow polymerase were added to the reaction mixture followed by incubation at 37°C for 40 minutes. The reaction was stopped by 2µl 0.5M EDTA and volume was made up to 100µl by adding TE. The pre-hybridized blot was then incubated with the radiolabeled probe for 16hrs at 65 °C. The blot was washed by wash buffer I (2X SSC, 1% SDS) twice for 30 min each at 65 °C and wash buffer II (0.5X SSC, 0.1% SDS) thrice for 20 min each at 65 °C. The membrane was exposed to Phosphor imager film, and the image was captured by Phosphorimager.

## 5.7 Purification of $H3V^{CTG}$ complexes

### 5.7.1 Immuno-precipitation of $H3V^{CTG}$ using CaRA107 strain

$H3V^{CTG}$ complexes were purified using mChIP method (JI *et al.* 2015; WIERER AND MANN 2016). CaRA107 overnight grown culture was inoculated in 500ml YPD. The culture was grown till 1-1.2OD. Next, the cells were pelleted at 5000 rpm at 4°C for 10 min. The pellet was washed with ice-cold 1X PBS twice and resuspended in 3ml of ice-cold lysis buffer (25mM HEPES pH=8, 2mM $MgCl_2$, 0.1mM EDTA, 0.5mM EGTA, 0.1% NP40, 300mM KCl, 15% glycerol, 1mM DTT, 0.2mM PMSF, 1mM NaF and protease inhibitor cocktail). Cells were lysed using homogenizer. The cell lysate was centrifuged at 4000 rpm for 10 min at 4°C. The supernatant was split into two fractions. The first fraction was sonicated using Bioruptor (Diagenode) in cycles of 10s on and 10s off bursts to obtain chromatin fragments of size 100-300 bp. After centrifuging (13,000 rpm, 10 min, 4°C),

chromatin fraction (supernatant) was distributed to Bead only ($BO^S$) and Immunoprecipitated material ($IP^S$). The second fraction was treated with 100 units/ml DNase in 1X DNase reaction buffer followed by incubation at room temperature for 15 min under constant rotation. Next, it was incubated at 4°C under constant rotation for 2hrs. After centrifuging (13,000 rpm, 10 min, 4°C), chromatin fraction was distributed to Bead only ($BO^D$) and Immunoprecipitated material ($IP^D$). DNA was purified from 50µl aliquot from both sonicated and DNase treated samples by phenol-chloroform extraction followed by ethanol precipitation. The pellet was resuspended in 30µl $dH_2O$. 5µl sample was loaded onto a 2% agarose gel to check the fragment size.

Protein A sepharose beads (Sigma, Cat. No. P9424-5ML) were washed with ice-cold PBS followed by overnight incubation with anti-V5 antibodies (Invitrogen, Cat. No. R6025) at 4°C under constant rotation (3.6 µg antibodies per 30 µl beads). Beads were washed five times with PBS and twice with lysis buffer (containing 150mM KCl). Antibody-coated beads were resuspended in an equivalent volume of lysis buffer to obtain 1:1 bead slurry.

60µl of antibody-coated bead slurry (30µl beads: 30µl lysis buffer) was used for each IP reaction ($IP^S$ and $IP^D$) and bead only ($BO^S$ and $BO^D$) reaction had 60µl protein A sepharose bead slurry without antibody. IP and BO reactions were incubated with the treated lysates overnight at 4°C under constant rotation. Next, beads were washed using lysis buffer six times. The protein complexes were eluted by directly boiling in lysis buffer for 10 min followed by electrophoresis on a 12% SDS-PAGE gel. Simultaneously two gels were run, one for western to check the presence of bait protein ($H3V^{CTG}$) and second for silver staining to check for interacting partners.

### 5.7.2 **Silver staining**

To perform silver staining, gels were fixed in fixing solution (55% methanol, 10% acetic acid, 35% $H_2O$) for 3hr or overnight. It was washed thrice with $H_2O$ for 10 min followed by incubation in 20 mg/100 ml Sodium thiosulphate solution for 1min. Next, the gel was rinsed thrice with autoclaved water thrice (20 sec each) followed by incubation in $AgNO_3$ solution (200mg/100ml) for 1 min followed by rinsing in water thrice for 20 sec each. Finally, it was incubated in developing solution (6 g/100 ml $Na_2CO_3$, 2 ml $Na_2S_2O_3$, and 75 µl of 37% formaldehyde) till the bands appear. The reaction was stopped with glacial acetic acid.

### 5.7.3 **Coomassie staining**

Coomassie staining was done to access protein loss at each step. Pellet fraction was resuspended in equal volume of lysis buffer as supernatant. 10µl of supernatant and pellet fractions collected at each centrifugation step was electrophoresed on 12% SDS-PAGE gel. The gel was stained in a staining solution (0.1% Coomassie Brilliant Blue R-250, 50% methanol, and 10% glacial acetic acid) for 30min followed by destaining (40% methanol and 10% glacial acetic acid) until a clear background was achieved.

**Table 3 *C. albicans* strains used in this study**

| Yeast strain | Genotype | Reference |
|---|---|---|
| SC5314 | Wild-type isolate | (GILLUM *et al.* 1984) |
| SN148 | *Δura3:: imm434/Δura3:: imm434 Δhis1:: hisG/Δhis1 ::hisG; Δarg4 :: hisG/Δarg4 ::hisG, Δleu2 :: hisG/Δleu2 :: hisG* | (NOBLE AND JOHNSON 2005) |
| LR107 | *Δhht1:: FRT=Δhht1 :: FRT* | (RAI 2014) |
| LR144 | *Δura3:: imm434/Δura3:: imm434 Δhis1:: hisG/Δhis1 ::hisG; Δarg4 :: hisG/Δarg4 ::hisG, Δleu2 :: hisG/Δleu2 :: hisG HHT1/HHT1-V5-HIS1* | (RAI 2014) |
| LR105 | *hht1::FRT/HHT1* | (RAI 2014) |
| LR113 | *Δura3:: imm434/Δura3:: imm434/CIp10 Δhis1:: hisG/Δhis1 ::hisG; Δarg4 :: hisG/Δarg4 ::hisG, Δleu2 :: hisG/Δleu2 :: hisG hht1::HIS1/hht1::NAT flp* | (RAI 2014) |
| LR114 | *Δura3:: imm434/Δura3:: imm434/CIp10 Δhis1:: hisG/Δhis1 ::hisG; Δarg4 :: hisG/Δarg4 ::hisG, Δleu2 :: hisG/Δleu2 :: hisG hht1::HIS1/hht1::NAT flp* | (RAI 2014) |
| LR115 | *Δura3:: imm434/Δura3:: imm434/CIp10 Δhis1:: hisG/Δhis1 ::hisG; Δarg4 :: hisG/Δarg4 ::hisG, Δleu2 :: hisG/Δleu2 :: hisG hht1::HIS1/hht1::FRT::HHT1::NATflp* | (RAI 2014) |
| CaRA101 | *HHT1V5::NAT/HHT1* | This study |
| CaRA106 | *HHT1V5::NAT/hht1::FRT* | This study |
| CaRA107 | *Δura3:: imm434/Δura3:: imm434 Δhis1:: hisG/Δhis1 ::hisG; Δarg4 :: hisG/Δarg4 ::hisG, Δleu2 :: hisG/Δleu2 :: hisG HHT1-V5::NAT/HHT1-V5 (HIS1)* | This study |
| CaRA110 | *Δura3:: imm434/Δura3:: imm434 Δhis1:: hisG/Δhis1 ::hisG; Δarg4 :: hisG/Δarg4 ::hisG, Δleu2 :: hisG/Δleu2 :: hisG NRG1pr-GFP::HIS1 BRG1pr-mCherry::ARG4* | This study |
| CaRA111 | *Δura3:: imm434/Δura3:: imm434/CIp10 Δhis1:: hisG/Δhis1 ::hisG; Δarg4 :: hisG/Δarg4 ::hisG, Δleu2 :: hisG/Δleu2 :: hisG NRG1pr-GFP::HIS1 BRG1pr-mCherry::ARG4* | This study |

**Table 4 Plasmids used in this study**

| Plasmid | Description |
|---|---|
| pRA01 | Cassette for tagging *HHT1* C-term with V5 using NAT marker |
| pRA04 | Cassette for tagging *NRG1pr* with GFP using HIS marker |
| pRA05 | Cassette for tagging *BRG1pr* with mCherry using ARG marker |

**Table 5 Oligonucleotide primers used in this study**

| Primer Name | Sequence (5'-3') |
|---|---|
| PJ 86 | ACAAGCTTATTGAGTGACGAAAA |
| PJ 87 | TTTACGGGTTGTTAAACCTTCGA |
| 6791V5-CFP | CGAGCTCTTAAGAGGTGAAAGATCTGGTAAG CCTATCCCTAACCCTCTCCTCGGTCTCGATTCT ACGTAAGACAGGATAAGATAGGAT |
| 6791V5-CRP | TCCCCGCGGGACTTCAAGATTATAATTAAAAC AAAG |
| 6791V52LFP | CTAATTTATGTGCTATTCATGCTAAAAGAGTT ACTATTCAAAAGAAAGATATGCAATTAGCTA GAAGATTAAGAGGTGAAAGATCT |
| RA1:6791V5NAT | CACTCATTTGCAATTTCAGTAATTTATTATTCT ACTTTTTAATATTTTTCCTTATGATTATCAACT CGGGCCCGGGACTGGATGGCGGCGTT |
| RA7: HHT1_US | CCACTTTGTCCTTAAACGTCG |
| RA8: NAT_promoter | CACGTCAAGACTGTCAAGGAG |
| RA9:pNRG1_FP_SacI | CGAGCTCGCAGATAAGGAATTATACACCAAC GAC |
| RA10:pNRG1_RP_SpeI | GACTAGTCGTTTGATTCTTAATGAAACTAGCA GG |
| RA11:pBRG1_FP_SacI | CGAGCTCGGACAGTAGAGTTTATCGTGGTTG |
| RA13:pBrg1_FP_SacII | GCCGCGGCGACAGTAGAGTTTATCGTGG |
| RA14_pBrg1_RP_nhe1 | GGCTAGCCGTAACAAGTATGGATGGAGAAAT AAC |
| RA15_pNRG1confirm_FP | CATTGTGTAGTTGCATTGTGAGTATAC |
| RA16:pNRG1confirm_RP | CAGTGAAAAGTTCTTCTCCCTTACTC |
| RA17:pBRG1confirm_FP | CATTATGTCGACTTTTCAGTTTAGCTTC |
| RA18:pBRG1confirm_RP | CCATATTATCTTCTTCACCTTTTGAAACCAT |

# REFERENCES

Alim, D., S. Sircaik and S. Panwar, 2018 The Significance of Lipids to Biofilm Formation in Candida albicans: An Emerging Perspective. Journal of Fungi 4**:** 140.

Alvarez, F. J., and J. B. Konopka, 2007 Identification of an N-acetylglucosamine transporter that mediates hyphal induction in Candida albicans. Molecular biology of the cell 18**:** 965-975.

Azadmanesh, J., A. M. Gowen, P. E. Creger, N. D. Schafer and J. R. Blankenship, 2017 Filamentation involves two overlapping, but distinct, programs of filamentation in the pathogenic fungus Candida albicans. G3: Genes, Genomes, Genetics 7**:** 3797-3808.

Bain, J. M., C. Stubberfield and N. A. Gow, 2001 Ura-status-dependent adhesion of Candida albicans mutants. FEMS microbiology letters 204**:** 323-328.

Basso, V., C. d'Enfert, S. Znaidi and S. Bachellier-Bassi, 2018 From Genes to Networks: The Regulatory Circuitry Controlling Candida albicans Morphogenesis.

Bereza-Malcolm, L. T., G. l. Mann and A. E. Franks, 2014 Environmental sensing of heavy metals through whole cell microbial biosensors: a synthetic biology approach. ACS synthetic biology 4**:** 535-546.

Biswas, S., P. Van Dijck and A. Datta, 2007 Environmental sensing and signal transduction pathways regulating morphopathogenic determinants of Candida albicans. Microbiology and Molecular Biology Reviews 71**:** 348-376.

Bleichrodt, R.-J., and N. D. Read, 2018 Flow cytometry and FACS applied to filamentous fungi. Fungal Biology Reviews.

Campos, E. I., A. H. Smits, Y.-H. Kang, S. Landry, T. M. Escobar *et al.*, 2015 Analysis of the histone H3. 1 interactome: a suitable chaperone for the right event. Molecular cell 60**:** 697-709.

Carlisle, P. L., M. Banerjee, A. Lazzell, C. Monteagudo, J. L. López-Ribot *et al.*, 2009 Expression levels of a filament-specific transcriptional regulator are sufficient to determine Candida albicans morphology and virulence. Proceedings of the National Academy of Sciences 106**:** 599-604.

Chatterjee, G., S. R. Sankaranarayanan, K. Guin, Y. Thattikota, S. Padmanabhan *et al.*, 2016 Repeat-associated fission yeast-like regional centromeres in the ascomycetous budding yeast Candida tropicalis. PLoS genetics 12**:** e1005839.

Chauvel, M., A. Nesseir, V. Cabral, S. Znaidi, S. Goyard *et al.*, 2012 A Versatile Overexpression Strategy in the Pathogenic Yeast Candida albicans: Identification of Regulators of Morphogenesis and Fitness. PLOS ONE 7**:** e45912.

Cheng, S., M. H. Nguyen, Z. Zhang, H. Jia, M. Handfield *et al.*, 2003 Evaluation of the roles of four Candida albicans genes in virulence by using gene disruption strains that express URA3 from the native locus. Infection and immunity 71**:** 6101-6103.

Chibana, H., N. Oka, H. Nakayama, T. Aoyama, B. Magee *et al.*, 2005 Sequence finishing and gene mapping for Candida albicans chromosome 7 and syntenic analysis against the Saccharomyces cerevisiae genome. Genetics 170**:** 1525-1537.

Cramer, R., and J. R. Perfect, 2009 Recent advances in understanding human opportunistic fungal pethogenesis mechanisms. Anaissie EJ, McGinnis MR, Pfaller MA. Clinical mycology. 2nd ed. Edinburg: Churchill Livingstone, Elsevier, Inc**:** 15-28.

Desai, J. V., and M. S. Lionakis, 2019 Setting Up Home: Fungal Rules of Commensalism in the Mammalian Gut. Cell host & microbe 25**:** 347-349.

Fox, E. P., C. K. Bui, J. E. Nett, N. Hartooni, M. C. Mui *et al.*, 2015 An expanded regulatory network temporally controls C andida albicans biofilm formation. Molecular microbiology 96**:** 1226-1239.

Gietz, R. D., and R. A. Woods, 2002 Transformation of yeast by lithium acetate/single-stranded carrier DNA/polyethylene glycol method, pp. 87-96 in *Methods in enzymology*. Elsevier.

Gillum, A. M., E. Y. Tsay and D. R. Kirsch, 1984 Isolation of the Candida albicans gene for orotidine-5′-phosphate decarboxylase by complementation of S. cerevisiae ura3 and E. coli pyrF mutations. Molecular and General Genetics MGG 198**:** 179-182.
Gow, N. A., A. J. Brown and F. C. Odds, 2002 Fungal morphogenesis and host invasion. Current opinion in microbiology 5**:** 366-371.
Grumaz, C., S. Lorenz, P. Stevens, E. Lindemann, U. Schöck *et al.*, 2013 Species and condition specific adaptation of the transcriptional landscapes in Candida albicans and Candida dubliniensis. BMC genomics 14**:** 212.
Gunasekera, A., F. J. Alvarez, L. M. Douglas, H. X. Wang, A. P. Rosebrock *et al.*, 2010 Identification of GIG1, a GlcNAc-induced gene in Candida albicans needed for normal sensitivity to the chitin synthase inhibitor nikkomycin Z. Eukaryotic cell 9**:** 1476-1483.
Heilmann, C. J., A. G. Sorgo, A. R. Siliakus, H. L. Dekker, S. Brul *et al.*, 2011 Hyphal induction in the human fungal pathogen Candida albicans reveals a characteristic wall protein profile. Microbiology 157**:** 2297-2307.
Homann, O. R., J. Dea, S. M. Noble and A. D. Johnson, 2009 A phenotypic profile of the Candida albicans regulatory network. PLoS genetics 5**:** e1000783.
Hull, C. M., R. M. Raisner and A. D. Johnson, 2000 Evidence for mating of the" asexual" yeast Candida albicans in a mammalian host. Science 289**:** 307-310.
Jackson, A. P., J. A. Gamble, T. Yeomans, G. P. Moran, D. Saunders *et al.*, 2009 Comparative genomics of the fungal pathogens Candida dubliniensis and Candida albicans. Genome research 19**:** 2231-2244.
Jain, N., K. V. Iyer, A. Kumar and G. Shivashankar, 2013 Cell geometric constraints induce modular gene-expression patterns via redistribution of HDAC3 regulated by actomyosin contractility. Proceedings of the National Academy of Sciences 110**:** 11349-11354.
Ji, X., D. B. Dadon, B. J. Abraham, T. I. Lee, R. Jaenisch *et al.*, 2015 Chromatin proteomic profiling reveals novel proteins associated with histone-marked genomic regions. Proceedings of the National Academy of Sciences 112**:** 3841-3846.
Kendrick, B., 2000 The Fifth Kingdom. Newburyport, pp. 373. Focus Publishing.
Klein, B. S., and B. Tebbets, 2007 Dimorphism and virulence in fungi. Current opinion in microbiology 10**:** 314-319.
Lane, S., C. Birse, S. Zhou, R. Matson and H. Liu, 2001 DNA array studies demonstrate convergent regulation of virulence factors by Cph1, Cph2, and Efg1 in Candida albicans. Journal of Biological Chemistry 276**:** 48988-48996.
Lay, J., L. K. Henry, J. Clifford, Y. Koltin, C. E. Bulawa *et al.*, 1998 Altered expression of selectable marker URA3 in gene-disrupted Candida albicans strains complicates interpretation of virulence studies. Infection and immunity 66**:** 5301-5306.
Legrand, M., P. Jaitly, A. Feri, C. d'Enfert and K. Sanyal, 2019 Candida albicans: An Emerging Yeast Model to Study Eukaryotic Genome Plasticity. Trends in Genetics.
Lim, C.-Y., R. Rosli, H. Seow and P. Chong, 2012 Candida and invasive candidiasis: back to basics. European Journal of Clinical Microbiology & Infectious Diseases 31**:** 21-31.
Lockhart, S. R., C. Pujol, K. J. Daniels, M. G. Miller, A. D. Johnson *et al.*, 2002 In Candida albicans, white-opaque switchers are homozygous for mating type. Genetics 162**:** 737-745.
Lohse, M. B., M. Gulati, A. D. Johnson and C. J. Nobile, 2018 Development and regulation of single-and multi-species Candida albicans biofilms. Nature Reviews Microbiology 16**:** 19.
Lu, Y., C. Su and H. Liu, 2014 Candida albicans hyphal initiation and elongation. Trends in microbiology 22**:** 707-714.

Magee, B., and P. Magee, 2000 Induction of mating in Candida albicans by construction of MTLa and MTLα strains. Science 289**:** 310-313.
Makhija, E., D. Jokhun and G. Shivashankar, 2016 Nuclear deformability and telomere dynamics are regulated by cell geometric constraints. Proceedings of the National Academy of Sciences 113**:** E32-E40.
Martin, R., D. Albrecht-Eckardt, S. Brunke, B. Hube, K. Hünniger *et al.*, 2013 A core filamentation response network in Candida albicans is restricted to eight genes. PloS one 8**:** e58613.
McNeil, M. M., S. L. Nash, R. A. Hajjeh, M. A. Phelan, L. A. Conn *et al.*, 2001 Trends in mortality due to invasive mycotic diseases in the United States, 1980–1997. Clinical infectious diseases 33**:** 641-647.
Miller, M. G., and A. D. Johnson, 2002 White-opaque switching in Candida albicans is controlled by mating-type locus homeodomain proteins and allows efficient mating. Cell 110**:** 293-302.
Moyes, D. L., D. Wilson, J. P. Richardson, S. Mogavero, S. X. Tang *et al.*, 2016 Candidalysin is a fungal peptide toxin critical for mucosal infection. Nature 532**:** 64.
Murad, A. M. A., P. R. Lee, I. D. Broadbent, C. J. Barelle and A. J. Brown, 2000 CIp10, an efficient and convenient integrating vector for Candida albicans. Yeast 16**:** 325-327.
Murad, A. M. A., P. Leng, M. Straffon, J. Wishart, S. Macaskill *et al.*, 2001 NRG1 represses yeast–hypha morphogenesis and hypha-specific gene expression in Candida albicans. The EMBO journal 20**:** 4742-4752.
Naseem, S., E. Araya and J. B. Konopka, 2015 Hyphal growth in Candida albicans does not require induction of hyphal-specific gene expression. Molecular biology of the cell 26**:** 1174-1187.
Nobile, C. J., E. P. Fox, J. E. Nett, T. R. Sorrells, Q. M. Mitrovich *et al.*, 2012 A recently evolved transcriptional network controls biofilm development in Candida albicans. Cell 148**:** 126-138.
Nobile, C. J., and A. D. Johnson, 2015 Candida albicans biofilms and human disease. Annual review of microbiology 69**:** 71-92.
Nobile, C. J., and A. P. Mitchell, 2005 Regulation of cell-surface genes and biofilm formation by the C. albicans transcription factor Bcr1p. Current Biology 15**:** 1150-1155.
Noble, S. M., B. A. Gianetti and J. N. Witchley, 2017 Candida albicans cell-type switching and functional plasticity in the mammalian host. Nature Reviews Microbiology 15**:** 96.
Noble, S. M., and A. D. Johnson, 2005 Strains and strategies for large-scale gene deletion studies of the diploid human fungal pathogen Candida albicans. Eukaryotic cell 4**:** 298-309.
Pande, K., C. Chen and S. M. Noble, 2013 Passage through the mammalian gut triggers a phenotypic switch that promotes Candida albicans commensalism. Nature genetics 45**:** 1088.
Pendrak, M. L., S. S. Yan and D. D. Roberts, 2004 Sensing the host environment: recognition of hemoglobin by the pathogenic yeast Candida albicans. Archives of biochemistry and biophysics 426**:** 148-156.
Pierce, C. G., and J. L. Lopez-Ribot, 2013 Candidiasis drug discovery and development: new approaches targeting virulence for discovering and identifying new drugs. Expert opinion on drug discovery 8**:** 1117-1126.
Rai, L. s., 2014 A CTG-clade specific histone H3 variant acts as a negative regulator of biofilm formation in *Candida albicans*, pp., JNCASR.

Riggle, P. J., K. A. Andrutis, X. Chen, S. R. Tzipori and C. A. Kumamoto, 1999 Invasive lesions containing filamentous forms produced by a Candida albicans mutant that is defective in filamentous growth in culture. Infection and immunity 67**:** 3649-3652.
San-Blas, G., L. Travassos, B. Fries, D. Goldman, A. Casadevall *et al.*, 2000 Fungal morphogenesis and virulence. Medical mycology 38**:** 79-86.
Selmecki, A., A. Forche and J. Berman, 2010 Genomic plasticity of the human fungal pathogen Candida albicans. Eukaryotic cell 9**:** 991-1008.
Shao, X., Q. Li, A. Mogilner, A. D. Bershadsky and G. Shivashankar, 2015 Mechanical stimulation induces formin-dependent assembly of a perinuclear actin rim. Proceedings of the National Academy of Sciences 112**:** E2595-E2601.
Shapiro, R. S., N. Robbins and L. E. Cowen, 2011 Regulatory circuitry governing fungal development, drug resistance, and disease. Microbiol. Mol. Biol. Rev. 75**:** 213-267.
Sudbery, P., N. Gow and J. Berman, 2004 The distinct morphogenic states of Candida albicans. Trends in microbiology 12**:** 317-324.
Sudbery, P. E., 2001 The germ tubes of Candida albicans hyphae and pseudohyphae show different patterns of septin ring localization. Molecular microbiology 41**:** 19-31.
Sudbery, P. E., 2011 Growth of Candida albicans hyphae. Nature Reviews Microbiology 9**:** 737.
Tao, L., H. Du, G. Guan, Y. Dai, C. J. Nobile *et al.*, 2014 Discovery of a "white-gray-opaque" tristable phenotypic switching system in Candida albicans: roles of non-genetic diversity in host adaptation. PLoS biology 12**:** e1001830.
Thompson, D. S., P. L. Carlisle and D. Kadosh, 2011 Coevolution of morphology and virulence in Candida species. Eukaryotic cell 10**:** 1173-1182.
Uppuluri, P., M. A. Zaldívar, M. Z. Anderson, M. J. Dunn, J. Berman *et al.*, 2018 Candida albicans dispersed cells are developmentally distinct from biofilm and planktonic cells. mBio 9**:** e01338-01318.
Wang, X., and B. C. Fries, 2011 A murine model for catheter-associated candiduria. Journal of medical microbiology 60**:** 1523.
Whiteway, M., and C. Bachewich, 2007 Morphogenesis in Candida albicans. Annu. Rev. Microbiol. 61**:** 529-553.
Wierer, M., and M. Mann, 2016 Proteomics to study DNA-bound and chromatin-associated gene regulatory complexes. Human molecular genetics 25**:** R106-R114.
Witchley, J. N., P. Penumetcha, N. V. Abon, C. A. Woolford, A. P. Mitchell *et al.*, 2019 Candida albicans morphogenesis programs control the balance between gut commensalism and invasive infection. Cell host & microbe 25**:** 432-443. e436.
Yue, H., J. Bing, Q. Zheng, Y. Zhang, T. Hu *et al.*, 2018 Filamentation in Candida auris, an emerging fungal pathogen of humans: passage through the mammalian body induces a heritable phenotypic switch. Emerging microbes & infections 7**:** 1-13.